Carbon dynamics at the river-estuarine transition: a comparison among tributaries of Chesapeake Bay.

Paul A. Bukaveckas

Center for Environmental Studies

Virginia Commonwealth University

Submitted to: Biogeosciences

August 3, 2021

revised December 10, 2021

Corresponding author: Paul Bukaveckas (pabukaveckas@vcu.edu)

Keywords: carbon, estuaries, mass balance CO_2 flux

Abstract

Sources and transformation of C were quantified using mass balance and ecosystem metabolism data for the upper segments of the James, Pamunkey and Mattaponi Estuaries. The goal was to assess the role of external (river inputs & tidal exchange) vs. internal (metabolism) drivers in influencing the forms and fluxes of C. C forms and their response to river discharge differed among the estuaries based on their physiographic setting. The James, which receives the bulk of inputs from upland areas (Piedmont and Mountain), exhibited a higher ratio of inorganic to organic C, and larger inputs of POC. The Pamunkey and Mattaponi receive a greater proportion of inputs from lowland (Coastal Plain) areas, which were characterized by low DIC and POC, and elevated DOC. I anticipated that transport processes would dominate during colder months when discharge is elevated and metabolism is low, and that biological processes would predominate in summer, leading to attenuation of C through-puts via de-gassing of CO_2. Contrary to expectations, highest retention of OC occurred during periods of high through-put, as elevated discharge resulted in greater loading and retention of POC. In summer, internal cycling of C via production and respiration was large in comparison to external forcing despite the large riverine influence in these upper estuarine segments. The estuaries were found to be net heterotrophic based on retention of OC, export of DIC, low GPP relative to ER, and a net flux of CO_2 to the atmosphere. In the James, greater contributions from phytoplankton production resulted in a closer balance between GPP and ER, with autochthonous production exceeding allochthonous inputs. Combining the mass balance and metabolism data with bioenergetics provided a basis for estimating the proportion of C inputs utilized by the dominant metazoan. The findings suggest that invasive catfish utilize 15% of total OM inputs and up to 40% of allochthonous inputs to the James.

Non-technical summary: Inland waters play an important role in the global carbon cycle by storing, transforming and transporting carbon from land to sea. Comparatively little is known about carbon dynamics at the river-estuarine transition. A study of tributaries of Chesapeake Bay showed that biological processes exerted a strong effect on carbon transformations. Peak carbon retention occurred during periods of elevated river discharge and was associated with trapping of particulate matter.

1. Introduction

Inland waters occupy a small proportion of surface area but play a disproportionately large role in global C cycling (Cole et al. 2007; Butman et al. 2016; Tranvik et al. 2018; Holgerson and Raymond 2016). River networks act as transport systems delivering C products of mineral weathering (DIC) and plant decomposition (DOC, POC) from the terrestrial realm to the coastal ocean (Meybeck 2003). Inland waters also function as reactors in which biotic and abiotic processes act to augment, transform or attenuate C fluxes. Aquatic primary production supplements terrestrial DOC and POC inputs, and by providing more labile forms of C, may facilitate the decomposition of older, recalcitrant terrestrial C. Decomposition of aquatic and terrestrial organic matter returns C to the atmosphere, which, along with C sequestration via sediment burial, results in the attenuation of C fluxes to the coastal zone (Richey et al. 2002; Vorosmarty et al. 2003; Middelburg and Herman 2007; Tranvik et al. 2009). Acting against these processes are fluvial forces that hasten through-puts of C and favor transport over processing. Along the flowpath from mountains to the sea, aquatic systems differ greatly in their capacity to attenuate C fluxes depending on factors such as water residence time, ecosystem metabolism and capacity for sediment accrual. Biological processes are expected to exert a stronger influence over C transport in lakes relative to streams and rivers, owing to their longer water residence time (Hotchkiss et al. 2018). Current efforts focus on understanding the net effect of inland waters on landscape scale fluxes of C. In this context, comparatively little attention has been focused on processes occurring at the river-estuarine transition.

The river-estuarine ecotone is defined by the transition from fluvial- to tidal-dominated forces, which results in a shift from unidirectional to bidirectional flow. In some settings, the point of transition may migrate in response to changing discharge conditions, with fluvial forces extending seaward during high discharge, and tidal forces gaining inland during periods of low freshwater inputs. Along the mid-Atlantic coast, the landward extent of tidal influence is delineated by a geologic feature (the Fall Line), a zone of rapid elevation change at the transition from upland (Piedmont) to lowland (Coastal Plain) physiographic regions. Below the Fall Line, hydrodynamics are estuarine in that they are subject to bi-directional flows associated with incoming and outgoing tides, whereas chemistry is riverine (freshwater). These conditions arise

because tidal forces propagate inland beyond the point where mixing of fresh and marine waters occurs.

Tidal freshwaters are a common feature of river-dominated estuaries throughout the world but have received relatively little attention in landscape-scale assessments of biogeochemical processes (Hoitink and Jay 2016; Ward et al. 2017; Jones et al. 2020). A key feature of tidal freshwaters is their prolonged residence time relative to non-tidal rivers (Jones et al. 2017). Water and materials exported during an out-going tide are returned on the incoming tide, thereby increasing residence time. For example, plankton community development in rivers is often constrained by short transit time (Soballe and Kimmel 1987; Pace et al. 1992; Basu and Pick 1996; Sellers and Bukaveckas 2003; Lucas et al. 2009), whereas the back and forth of tidal flows reduces net seaward movement resulting in longer transit time (Shen and Lin 2006; Qin and Shen 2017). Bi-directional flows in tidal freshwaters create more favorable water residence time conditions (relative to non-tidal rivers) that allow for the development of phytoplankton communities and the potential for greater biological influence on C forms and retention. Our prior work in the James Estuary has documented higher rates of ecosystem metabolism in the tidal freshwater segment relative to adjacent riverine and lower estuarine segments (Tassone and Bukaveckas 2019; Bukaveckas et al. 2020). The occurrence of a chlorophyll-a and productivity maxima in the tidal fresh zone was attributed to longer water residence time and proximal nutrient inputs from riverine and local point sources (Bukaveckas et al. 2011; Qin and Shen 2017). Other studies have also documented tidal freshwaters as potential biogeochemical hotspots (Vincent et al. 1996; Muylaert et al. 2005; Hoffman et al. 2008; Lionard et al. 2008; Amann et al. 2015; Young et al. 2021; Xu et al. 2021).

The goal of this study was to assess the relative importance of external (river inputs & tidal exchange) vs. internal (metabolism) drivers in influencing C forms and retention in the upper estuary. Long water residence time and high rates of ecosystem metabolism in the tidal fresh zone were expected to favor the importance of internal processes over external hydrologic forces in regulating C throughputs. During periods of low river discharge, longer water residence in the estuary allows accrual of phytoplankton biomass and greater GPP, which may result in net autotrophy and greater export of organic C relative to DIC. Alternatively, the production of autochthonous labile C may facilitate mineralization of allochthonous C inputs (“priming

100 effect") resulting in CO_2 release and attenuation of organic and total C exports (Bianchi 2011;
101 Steen et al. 2015; Ward et al. 2016). During periods of elevated discharge, freshwater
102 replacement time in the upper estuary is short, thereby favoring transport over retention.
103 However, our recent work has shown that the bulk of N and P retention in the tidal fresh zone of
104 the James Estuary occurs during periods of high sediment loading (Bukaveckas et al. 2018).
105 Although retention of dissolved N and P was highest during peak production in summer, the
106 trapping of particulate N and P in winter accounted for the bulk of total N and P retention. These
107 findings suggest that retention of particulate and total C may be highest during periods of
108 elevated river discharge.

109 In this study, mass balance results and ecosystem metabolism data were used to assess C inputs,
110 outputs, transformation and retention in the upper estuarine segments of two Chesapeake Bay
111 tributaries. For the James Estuary, these data are also used to estimate allochthonous and
112 autochthonous inputs and to assess constraints on food web energetics.

113

114 ## 2. Methods

115 2.1 Study Sites. This study focuses on the upper segments of the two southern tributaries of
116 Chesapeake Bay (James and York Estuaries), the latter of which is comprised of two sub-
117 estuaries (Pamunkey and Mattaponi). This is the third in a series of papers that rely in part on
118 comparisons among these estuaries to draw inferences about processes occurring at the river-
119 estuarine transition. Previous papers focused on the influence of storm events on river and
120 estuarine metabolism and water quality (Bukaveckas et al. 2020), and on factors regulating water
121 clarity and primary production (Henderson & Bukaveckas 2021). The proximity of the estuaries
122 facilitated frequent sampling (1-2 week intervals) that is needed to characterize C fluxes. The
123 study reach within the James Estuary is the tidal fresh segment, which extends 88 km from the
124 Fall Line (Richmond, VA) to the confluence with the Chickahominy River, and accounts for
125 ~50% of the length of the estuary. Study reaches for the Pamunkey and Mattaponi Estuaries
126 encompassed the tidal fresh and oligohaline segments, extending 86 km to their confluence with
127 the York Estuary. A key difference among the estuaries is their geographic setting across
128 lowland (Coastal Plain) and upland (Piedmont and Mountain) areas (Figure 1). Freshwater
129 inputs to the James tidal fresh segment are largely (90%) derived from upland sources (i.e.,

above the Fall Line), whereas local (Coastal Plain) tributaries contribute ~10% (based on the proportion of contributing area below the Fall Line). By contrast the Pamunkey and Mattaponi Estuaries receive a greater proportion of freshwater inputs from local (Coastal Plain) sources (36% and 51%, respectively). Higher sediment yield from upland sources should result in greater POC inputs to the James relative to the Pamunkey and the Mattaponi. I also expected that higher GPP and R in the phytoplankton-dominated James Estuary would exert a stronger influence on C transformations relative to the Pamunkey and Mattaponi, which are dominated by submerged and emergent aquatic vegetation. Lastly, extensive floodplain and wetland areas along the Pamunkey and Mattaponi would be expected to contribute greater DOC inputs relative to the James.

2.2 Data Collection. For the James, I am able to present a relatively complete C budget inclusive of Fall Line loads, local tributary inputs and tidal fluxes of inorganic and organic fractions (DIC, DOC, POC). These results are based on data collected from river and estuarine stations over a 10-year span (2010-2019). For the Pamunkey and Mattaponi, the scope is more limited both in the time span over which data were collected (2017-2019) and, due to the lack of data on Fall Line DIC and chloride inputs, which precludes estimation of tidal exchange using Cl mass balance. For the James and Pamunkey, previously published estimates of GPP and ER derived from in situ diel oxygen cycles are used to assess their effect on C transformations. Seasonal patterns in CO_2 concentrations and air-water exchange are provided for all three estuaries.

2.3 C Inputs & Estuarine Export. External C loads for the three estuaries were derived from (a) measured discharge and concentration at the Fall Line, and (b) estimated contributions from ungauged tributaries below the Fall Line. Fall Line loads were based on data collected by the USGS at gauging stations located on the James, Pamunkey and Mattaponi Rivers. Fall Line samples were collected at approximately monthly intervals, with supplemental samples collected during periods of high discharge. Approximately 200 measurements of DOC and POC were obtained at each of the gauging sites over the 10-year span (Table 1), along with continuous measurements of river discharge. For the James, the USGS data were supplemented by measuring DIC and Cl at the Fall Line at 1-2 week intervals during 2012-2019 (189 samples collected). Seasonal, inter-annual and discharge-dependent variation in riverine C concentrations was analyzed using Generalized Additive Models (see Statistics). The models were used to

predict daily concentrations at each site, and, in combination with daily discharge, to derive daily loading values at the Fall Line. Local (ungauged) runoff was estimated as a constant fraction of the daily Fall Line discharge based on the proportion of catchment area represented by tributaries entering below the Fall Line. Daily concentrations were used in combination with Fall Line discharge, below Fall Line discharge, and total discharge to derive daily input and export fluxes. Daily fluxes were summed over the budget interval (typically 1-2 weeks) and used, in conjunction with the change in mass of Cl in the estuary between the start and end of each interval, to solve for the net tidal flux of Cl.

$$\textit{Estuary Cl Mass}_{t+1} = \textit{Estuary Cl Mass}_t + \textit{Riverine Cl} - \textit{Export Cl} \pm \textit{Net Tidal Cl} \quad (1)$$

The mass of Cl required to balance each budget interval was used in combination with measurements of Cl concentrations in tidal inflow and outflow, as represented by stations located on either side of the seaward boundary of our study reach (JMS69 and JMS56), to derive the effective volume of tidal exchange. This represents the volume of "new" water entering the study reach from the lower estuary with each tidal cycle. The James has an elongate shape that is typical of estuaries that occupy flooded river valleys. The back and forth of tidal flows means that the bulk of the water leaving on an outgoing tide returns on the subsequent incoming tide, and only a small proportion of the large tidal flux is "new" water. For the James, the effective volume of exchange is equivalent to 8% of the tidal prism (Bukaveckas and Isenberg 2013). For this study, estimates of the volume of tidal exchange were derived for each budget interval (N = 309 for 2011-19). The effective volume of exchange was used along with measured C concentrations of tidal inflows and outflows to determine the net exchange of C at the seaward boundary of the study reach. Net tidal fluxes for each budget interval were aggregated to monthly values and presented as daily areal values for comparison to riverine input and export fluxes. Lastly, monthly estimates of estuarine C retention were derived based on the difference between input and output fluxes taking into account changes in mass storage within the estuary.

$$\textit{Estuary C Mass}_{t+1} = \textit{Estuary C Mass}_t + \textit{Riverine C} - \textit{Export C} \pm \textit{Net Tidal C} \pm \textit{Retention} \quad (2)$$

For DIC, our estimation of retention also took into account air-water CO_2 exchange (see below).

2.5 Estuarine Metabolism. Previously published estimates of Gross Primary Production (GPP) and Ecosystem Respiration (ER) were used to assess internal C transformations for the James

and Pamunkey (Bukaveckas et al. 2020). Rates of metabolism were derived from continuous (15 min) monitoring of dissolved oxygen at stations located within our study segments of the James and Pamunkey (Figure 1). The James monitoring station is located at the VCU Rice Center Research Pier, approximately 2 km from our JMS75 sampling location. The Pamunkey station (White House Landing) is operated by the Virginia Institute of Marine Science and located near the mid-point of our study segment. Similar equipment (YSI 6600 or EXO sondes) and protocols are used at the two stations including routine (2-3 week) maintenance and calibration of sondes as per manufacturer recommendations. Daily GPP and ER were derived using the single-station open-water method. Following Caffrey (2003; 2004), 15-minute DO measurements were smoothed to 30-minute averages and multiplied by water depth to obtain areal rates of oxygen flux at 30 minute intervals throughout the day.

$$O_2 \text{ flux } (g\ O_2\ m^{-2}\ d^{-1}) = (DO_{t2}\text{-}DO_{t1}) * \text{Water Depth} - AE \quad (3)$$

Atmospheric exchange (AE) was derived at 30-minute intervals based on water column DO saturation and a generic estuarine gas transfer coefficient. A previous analysis using 23 years of station data for the James showed that estimates of atmospheric exchange derived from oxygen saturation and the fixed gas transfer coefficient were not significantly different from exchange coefficients derived using variable water velocity and wind speed (Tassone and Bukaveckas 2019). ER was derived by extrapolating nightly O_2 fluxes to a 24-hour period. GPP was derived as the sum of daytime oxygen production and ER during daylight hours. Oxygen-based values were converted to C assuming a photosynthetic quotient of 1.2 and a respitory quotient of 1.

2.6 Sampling and Analysis. Methods were described previously (Bukaveckas et al. 2011; Bukaveckas et al. 2020; Henderson and Bukaveckas 2021) and are summarized here. Data were collected from 4 stations in the James tidal fresh segment, 3 stations in each of the Pamunkey and Mattaponi study reaches, and one tributary stream (Kimages Creek) located at the VCU Rice Center (Figure 1; Table 1). Estuarine sites were sampled by boat in the main channel except in the upper, narrow sections of the Pamunkey and Mattaponi where samples were collected from shore in areas of active flow. Owing to vertically well-mixed conditions (no temperature or salinity stratification) water samples and in situ measurements were obtained near the surface (~0.5 m). Water temperature and salinity were measured using a YSI Pro DDS sonde. The partial pressure of carbon dioxide in water and air was measured in the field using a PP Systems

EGM 4 portable infrared CO_2 analyzer calibrated at 0 and 2000 ppm. Water samples were analyzed for chlorophyll-a (CHLa), POC, DIC, DOC and Cl. Samples for CHLa and POC were filtered through Whatman GF/A glass filters (0.5-µm nominal pore size). Filters for CHLa analyses were extracted for 18 h in buffered acetone and analyzed on a Turner Design TD-700 Fluorometer (Arar and Collins 1997). Filters for POC analysis were dried at 60 C for 48 h, fumed with HCl to remove inorganic carbon and analyzed on a Perkin–Elmer CHN analyzer. Chloride concentrations were determined using a Skalar segmented flow analyzer by the ferriccyanide method (APHA 1998). Samples for DIC and DOC were filtered in the field through Whatman GF/A filters and analyzed using a Shimadzu TOC analyzer.

2.7 Air-Water CO_2 Fluxes. Air-water exchange of CO_2 was calculated using the equation from Cai and Wang (1998):

$$\text{Flux } CO_2 = K_T K_H (pCO_{2\text{-water}} - pCO_{2\text{-air}}) \quad (4)$$

where K_T is the gas transfer velocity, K_H is the solubility constant and pCO_2 is the partial pressure of CO_2 in water and air. The solubility constant was derived according to the equation of Weiss (1974) taking into account water temperature and salinity recorded at the time of CO_2 measurement. Gas transfer velocities were initially derived from daily average wind speed (U10 corrected) measured at the VCU Rice Center Research Pier (James) and the Taskinas Creek NERR station (Pamunkey and Mattaponi). Gas transfer velocities derived from wind speed generally fell within the range of 1 to 1.5 m d^{-1}, which is low in comparison to the global average (5.7 m d^{-1}, Raymond et al. 2017) and to values that are considered appropriate for large rivers (4.3 m d^{-1}, Alin et al. 2011; Reiman and Xu 2019). Based on these considerations, a value of 4.3 m d^{-1} was used for all calculations (see Discussion for further consideration of gas transfer velocities).

2.8 Statistics. Generalized Additive Models (GAMs) were used to model river and estuarine C and Cl concentrations based on discharge, day of year (to capture seasonal patterns) and decimal date (to depict inter-annual variation). GAMs are gaining increasing usage for modeling water chemistry due to their ability to account for non-linear effects and to fit trends of a form that is not known *a priori* (Morton & Henderson 2008; Murphy et al. 2019; Yang and Moyer 2020; Wiik et al. 2021). The GAM analysis was performed using the "mgcv" package in R (Wood 2006). The package default thin plate regression spline was used to depict the effect sizes of

discharge and decimal date; a cyclic cubic regression spline was used to depict seasonal effects. The default output for the effect size was shifted to center on the mean of the modeled dependent variable to show the response of the GAM model within the range of dependent variable values.

3. Results

3.1 Estuarine Hydrology

The James, Pamunkey and Mattaponi Rivers exhibit similar hydrographs with highest monthly average discharge during January-May and lowest discharge in July-November (Figure 2). Average monthly discharge in winter-spring is approximately 4-fold higher in comparison to summer-fall. Median freshwater replacement times (FRT), taking into account Fall Line inputs plus local (ungauged) tributaries, were 30 d (James), 46 d (Mattaponi) and 60 d (Pamunkey) during the period of study. The mass of Cl in the James tidal fresh segment varied by >20-fold from seasonal minimum values during high discharge (~7 mg L^{-1}) to peak values (>100 mg L^{-1}) during summer base flow (Figure 3). Despite the large seasonal variation, Cl changed relatively slowly within the estuary (median = 0.5 % d^{-1}). The gradual change in estuarine Cl belies the underlying dynamics in which input and output fluxes largely offset. Riverine inputs (Fall Line plus local) ranged from 1 to 3 g Cl m^{-2} d^{-1} over the seasonal cycle. These displaced a larger mass of Cl (export = 2-5 g Cl m^{-2} d^{-1}) owing to higher Cl concentrations in the estuary relative to river inputs. In late summer (August-October), the development of strong Cl gradients across the seaward boundary of the study reach resulted in high rates of Cl gain and loss via tidal exchange (up to 10-20 g Cl m^{-2} d^{-1}). As the lower tidal fresh segment accounts for the bulk of total volume (80%), increases in Cl at the seaward end of the study reach had a large effect on estuarine Cl mass. These seasonal increases in estuarine Cl were most pronounced in summers with low freshwater inputs (e.g., 2012, 2017, 2019). By volume, the effective tidal exchange derived from the Cl mass balance was equivalent to 7.4% (median) and 14 ± 1% (mean and SE) of the tidal prism.

3.2 Discharge Effects on River and Estuarine C

Discharge was a significant factor influencing riverine C concentrations, though the strength of these effects differed among C fractions and among the three tributaries. Increasing discharge

was associated with increasing river DOC in the Mattaponi (from 6 to 12 mg L^{-1}) and Pamunkey (from 5 to 9 mg L^{-1}), but had little effect on James River DOC, which was generally low over the range of observed discharge (3-4 mg L^{-1}; Figure 4). Generalized Additive Models incorporating discharge, seasonal and inter-annual variation accounted for 50 to 81% of the variation in river DOC (Table 2). Seasonal patterns were characterized by peak river DOC in summer and minimum values in spring, with a seasonal range of 2-3 mg L^{-1} (Supplemental Figure 1). Increasing discharge was associated with large increases of POC in the James River (from 1 to 20 mg L^{-1}; Figure 4). Discharge accounted for the bulk of the variation in James River POC (71%) with little additional variation explained by season or inter-annual effects (76% for full model). The effects of discharge on river POC were weaker in the Mattaponi and Pamunkey, where concentrations were generally low over the range of discharge (<2 and <4 mg L^{-1}, respectively). Models incorporating discharge, seasonal and inter-annual variation accounted for 38% and 51% (respectively) of the variation in river POC at these sites (Supplemental Figure 2). Increasing discharge was associated with large decreases in DIC of the James River (from 20 to 1 mg L^{-1}; Figure 4). The GAM analysis accounted for 44% of the variation in DIC at this site (no river DIC data for Pamunkey and Mattaponi). Overall, increasing discharge resulted in higher DOC concentrations in the Pamunkey and Mattaponi Rivers, higher POC concentrations in the James River, and lower DIC concentrations in the James River.

Although increases in discharge had a positive effect on riverine DOC and POC, estuarine concentrations were only weakly, and in some cases negatively affected by increasing discharge (Figure 5). In the James, estuarine DOC concentrations were typically higher than riverine values (Supplemental Figure 3), such that increases in river discharge resulted in a reduction in estuarine DOC (from 7 to 2 mg L^{-1}). In the Pamunkey and Mattaponi, increasing discharge had little effect on estuarine DOC as estuarine concentrations were similar to river concentrations (Figure 5). Discharge was not a significant predictor of variation in DOC for the Pamunkey and Mattaponi Estuaries (Table 2). Seasonal and inter-annual effects were also weak, resulting in a low proportion of variation in estuarine DOC explained by the GAMs (13-27%). Similar findings for POC showed weak seasonal, inter-annual and discharge dependent effects and a low proportion of explained variation for the Pamunkey and Mattaponi Estuaries (40% and 14%, respectively). In contrast, POC concentrations in the James Estuary were strongly influenced by season, with predicted concentrations rising from 1 to 2 mg L^{-1} during winter to summer. POC

309 concentrations were negatively related to discharge, declining by ~0.5 mg L^{-1} over the lower
310 range of discharge (up to 400 m^3 s^{-1}). The overall model accounted for 75% of the variation in
311 POC for the James Estuary. Increasing discharge had a significant negative effect on DIC in all
312 three estuaries, which decreased by 5-6 mg L^{-1} over the observed range of discharge. Seasonal
313 and inter-annual effects on estuarine DIC were weaker; the full models accounted for 68-76% of
314 the variation in estuarine DIC. Overall, these findings show that river discharge had strong
315 negative effects on estuarine DIC, but little influence on estuarine DOC and POC. Significant
316 seasonal variation in POC was observed in the James, but not the Pamunkey or Mattaponi.

317 3.3 Estuarine pCO_2

318 GAM analysis revealed significant seasonal and discharge-dependent variation in estuarine pCO_2
319 (Table 2). The effects of discharge on estuarine pCO_2 differed among the 3 tributaries (Figure
320 6). In the Pamunkey and Mattaponi, there was little effect of discharge, except in the upper
321 quartile of the range, which was associated with rising estuarine pCO_2. In the James, estuarine
322 pCO_2 increased linearly over the lower one-third range of discharge, and thereafter plateaued.
323 The Mattaponi and Pamunkey exhibited large seasonal variations in estuarine pCO_2. Peak
324 summer concentrations (~2600 ppmv) were two-fold higher in comparison to winter minimum
325 values (~1200 ppmv;). A more complex seasonal pattern was observed in the James with bi-
326 model peaks in spring and fall (850 and 1250 ppmv, respectively) bracketing low concentrations
327 in mid-summer. In summer, significantly lower pCO_2 was observed at sites located at the CHLa
328 maximum (JMS75 = 789 ppmv, JMS69 = 644 ppmv) relative to stations in the upper tidal fresh
329 segment (JMS99 = 1007 ppmv) and the most seaward station (JMS56 = 909 ppmv; $p < 0.01$).
330 The two stations located at the CHLa maximum were the only sites to exhibit periodic under-
331 saturation of pCO_2 (Supplemental Figure 4). The low values at these stations were not observed
332 in winter. There was little longitudinal variation in pCO_2 among stations in the Pamunkey and
333 Mattaponi. Overall, annual average concentrations in the Pamunkey (2010 ± 117 ppmv) and
334 Mattaponi (1900 ± 120 ppmv) were more than 2-fold higher relative to the James (784 ±77
335 ppmv). Higher pCO_2 concentrations in the Pamunkey and Mattaponi estuaries were associated
336 with larger air-water CO_2 fluxes (2.97 ± 0.17 and 2.77 ± 0.17 g C m^{-2} d^{-1}, respectively) relative
337 to the James (0.87 ± 0.05 g m^{-2} d^{-1}; Figure 7). Strong seasonal patterns were observed in the

Pamunkey and Mattaponi with monthly average fluxes ranging from 1-2 g m^{-2} d^{-1} in winter to 3-4 g m^{-2} d^{-1} in summer, whereas fluxes from the James were similar year-round (~1 g m^{-2} d^{-1}).

3.4 C Fluxes & Retention

C fluxes into and out of the James Estuary varied seasonally (Figure 8). DOC inputs followed expected seasonal patterns with peak values (1-2 g m^{-2} d^{-1}) during months with elevated discharge (January-May) and minimum values (~0.3 g m^{-2} d^{-1}) during predominantly low discharge in July-November. Seasonal variation in DOC inputs was closely matched by export fluxes. Net tidal fluxes were negligible by comparison (-0.03 ± 0.01 g m^{-2} d^{-1}) owing to small differences in concentration across the segment boundary. Monthly DOC retention ranged from -0.30 to 0.12 g m^{-2} d^{-1}, and was generally negative, indicating net export of DOC. On an annual basis, the DOC balance was -0.10 ± 0.02 g m^{-2} d^{-1}, with export exceeding inputs by 11 ± 5%. Riverine inputs of POC varied seasonally with highest values in January-May (0.5 to 1.9 g m^{-2} d^{-1}) and generally low values in June-December (< 0.3 g m^{-2} d^{-1}). By contrast, estuarine export of POC was consistently low throughout the year (< 0.5 g m^{-2} d^{-1}). As a result, POC retention was highest in January-May (0.3 to 1.5 g m^{-2} d^{-1}). Net tidal fluxes were positive indicating a loss of POC with each tidal cycle, but these fluxes were small (0.09 ± 0.03 g m^{-2} d^{-1}) in comparison to river inputs. On an annual basis, the net retention of POC was 0.59 ± 0.11 g m^{-2} d^{-1}, corresponding to 72 ± 4% of inputs. DIC input and output fluxes followed a similar pattern as for DOC, with peak values in months with high discharge. Taking into account estuarine export and atmospheric fluxes, the James was a net source of DIC with losses (4.25 g m^{-2} d^{-1}) exceeding inputs (2.82 g m^{-2} d^{-1}) by 51%.

Our mass balance analysis does not explicitly consider the role of point source inputs in the estuarine C budget. Point sources that discharge to the tidal fresh segment of the James are principally wastewater treatment plants, and some industries associated with the Richmond metro area. The volume of effluent discharged to the James is small (annual average = 15-21 m^3 s^{-1} during 2007-14) in comparison to annual average river discharge (~225 m^3 s^{-1}). But as effluent may contain elevated C concentrations, point sources could potentially contribute an appreciable fraction of C inputs. Point sources typically do not report C concentrations as part of their effluent monitoring, therefore we carried out a 2-year study of DIC, DOC and POC concentrations in effluent from the largest point source (City of Richmond WWTP). Effluent

368 POC concentrations (1.54 ± 0.13 mg L^{-1}) were comparable to riverine values, whereas effluent
369 DOC (13.1 ± 1.2 mg L^{-1}) and DIC (22.7 ± 1.6 mg L^{-1}) were two-fold higher relative to riverine
370 concentrations. These values were extrapolated to all point source inputs to the James as a first
371 approximation of their potential importance to the estuarine C budget. Daily average POC loads
372 from point sources (0.02 g m^{-2} d^{-1}) were too small to appreciably affect our estimate of estuarine
373 POC retention. Point source inputs of DOC (0.21 g m^{-2} d^{-1}) and DIC (0.36 g m^{-2} d^{-1}) were
374 equivalent to 23% and 12% (respectively) of riverine inputs. Taking into account point source
375 contributions, the mass balance shows that the James tidal fresh segment is a net sink for DOC
376 (0.12 g m^{-2} d^{-1}) and POC (0.61 g m^{-2} d^{-1}) and a net source of DIC (1.07 g m^{-2} d^{-1}). Overall, the
377 James tidal fresh segment was nearly in balance (within 6%) for total C inputs and outputs.

378 Annual average DOC loads to the Pamunkey (0.67 ± 0.11 g m^{-2} d^{-1}) and Mattaponi (0.89 ± 0.12
379 g m^{-2} d^{-1}) were similar to the James (0.91 ± 0.12 g m^{-2} d^{-1}) on an areal basis. Seasonal variation
380 in DOC inputs followed patterns in discharge with peak values (0.7 – 1.7 g m^{-2} d^{-1}) in winter-
381 spring and minimum values (0.2 – 0.7 g m^{-2} d^{-1}) in summer-fall (Figure 9). Export fluxes closely
382 matched river inputs on a seasonal basis, and balanced to within 10% on an annual basis.
383 Riverine POC inputs to the Pamunkey and Mattaponi (0.17 ± 0.03 and 0.14 ± 0.02 g m^{-2} d^{-1},
384 respectively) were considerably lower relative to the James (0.81 ± 0.15 g m^{-2} d^{-1}). For the
385 James, POC inputs were nearly equal to DOC inputs, whereas for the Pamunkey and Mattaponi,
386 DOC accounted for the bulk of OC inputs (79% and 86%, respectively). Export of POC from
387 the Pamunkey and Mattaponi matched inputs to within 10% on an annual basis.

388 3.5 Estuarine Metabolism

389 Rates of GPP and ER were compared to standing stocks (areal values) of DIC and POC to assess
390 the potential influence of C fixation and remineralization on estuarine C concentrations (Figure
391 10). In the James, GPP and ER followed expected seasonal patterns with peak values (3.5 – 4.0
392 g C m^{-2} d^{-1}) during June-September and low values (<1 g C m^{-2} d^{-1}) in colder months. GPP and
393 ER tracked closely throughout the year, with ER exceeding GPP in colder months, and being
394 equal, or occasionally smaller (June-July) than GPP in warmer months. C fluxes associated with
395 GPP and ER were small in comparison to ambient concentrations of DIC, which ranged from 30
396 to 40 g m^{-2}. By contrast, POC production via GPP was comparable to ambient concentrations of
397 POC, which ranged from 3 g m^{-2} in colder months to 6 g m^{-2} in warmer months. Metabolism of

the Pamunkey Estuary was lower and more heterotrophic in comparison to the James. ER varied seasonally from 0.5 to 1.8 g C m^{-2} d^{-1}, whereas GPP was persistently low throughout the year (< 0.5 g C m^{-2} d^{-1}). Standing stocks of DIC were large by comparison, ranging from 10 to 40 g m^{-2}. GPP was small in comparison to standing stocks of POC (3 to 5 g m^{-2}).

4.0 Discussion

4.1 Riverine C Inputs & Estuarine Concentrations

An analysis of C dynamics in the upper portions of the James, Mattaponi and Pamunkey estuaries revealed differences in dominant forms of C and variable responses to changes in river discharge. The James was dominated by products of mineral weathering as DIC accounted for 73% of total C with smaller contributions from DOC (20%) and POC (7%). By contrast, organic forms accounted for a larger fraction (49%) of total C in the Pamunkey and Mattaponi. These differences are attributed to variable contributions from local (Coastal Plain) vs. upland (Mountain and Piedmont) runoff. The James Estuary receives inputs from a large catchment with the bulk of runoff (90%) derived from above the Fall Line. By contrast, the Pamunkey and Mattaponi Estuaries receive a greater proportion of their inputs from local tributaries situated within the Coastal Plain. Local floodplains and tidal marshes contribute DOC, while the predominantly sandy soils of the Coastal Plain have low capacity for retaining DOC, and contribute little DIC. Differences in source waters may also account for contrasting response in river and estuarine C to high discharge events. Larger increases in POC were observed during discharge events in the James, relative to the Pamunkey and Mattaponi. Prior studies documented higher sediment yields from Mountain and Piedmont regions in comparison to the Coastal Plain (Gellis et al. 2009). In the James River, changes in C concentrations with increasing discharge were asynchronous as DIC was negatively related to discharge, whereas POC showed a positive relationship. These findings suggest that DIC export from the watershed is limited by weathering rates (source limited) whereas POC export is transport limited (Wymore et al. 2021). For DIC, this resulted in a dilution response in both the river and estuary, whereas high discharge resulted in a flushing response (enrichment) of POC in the river and estuary. Dilution of estuarine DIC during high discharge was also reported in the nearby Delaware Estuary and linked to reductions in acid neutralizing capacity and greater sensitivity to acidification (Joesef et al. 2017). For DOC, a strong flushing response was observed in the

Pamunkey and Mattaponi Rivers, but not the James. Higher DOC concentrations following storm events has been attributed to greater leaching from soils due to higher water elevation and soil inundation (Zarnetske et al. 2018; Patrick et al. 2020). The extensive wetlands and floodplains along the Mattaponi and Pamunkey likely serve as source areas for DOC. Prior work showed that differences in source waters played a role in determining underwater light conditions in these estuaries, as light attenuation in the James was strongly regulated by suspended particulate matter, whereas dissolved organic matter had a greater role in attenuating light in the Pamunkey and Mattaponi estuaries (Henderson and Bukaveckas 2021). Overall, our findings showed strong concentration-discharge relationships in riverine waters, whereas estuarine responses were weaker and more variable. Inter-estuarine differences in C forms and response to discharge were linked to differences in the physiographic setting of the estuarine catchments.

4.2 C Mass Balance

The tidal freshwater segment of the James Estuary was a net sink for POC and DOC, and a net source of DIC. On an annual basis, external organic matter inputs were attenuated by 28% (±3) within the tidal fresh segment. The mass balance indicates that a high proportion (72%) of POC inputs were retained in the tidal fresh segment and that retention of POC accounted for the bulk (84%) of organic matter retention. Amann et al. (2012) similarly documented high retention of POC in tidal freshwaters of the River Elbe. The transition from fluvial to tidal conditions favors the settling of suspended particulate matter, which contained ~10-20% organic matter (Bukaveckas et al. 2019). Peak retention occurred during periods of elevated discharge when inputs of particulate matter to the estuary were highest. Our findings do not support the view that inlands waters function primary as transport systems ("pipes") during periods of elevated discharge (Zarnetske et al. 2018) as the bulk of organic matter retention occurred during high flows in winter, and was associated with the retention of particulates. High retention of particulate C is consistent with prior results showing that peak retention of N and P occurred during colder months with elevated river discharge (Bukaveckas and Isenberg 2013). Retention of dissolved N and P was highest during low discharge in summer, but this accounted for a relatively small proportion of total N and P retention on an annual basis. For C, as for N and P, the mass of particulate matter delivered to the estuary during high discharge appears to be the

458 most important determinant of the amount retained within the estuary. The counter-intuitive
459 finding that peak retention occurs during periods of high transport (when "pipe" conditions
460 might prevail) is based on a consideration of the fate of both dissolved and particulate organic
461 matter, as the former largely passes through, while the latter is highly retained. The retention of
462 particulate matter reflects the underlying hydrodynamics of estuaries, and lakes, where the rapid
463 dissipation of fluvial forces promotes high retention of particulate matter during periods of
464 elevated discharge.

465 For the James, atmospheric losses were a small component of the C budget, equivalent to 18% of
466 riverine total C inputs and 15% of total C export. Volta et al. (2016) similarly report that CO_2
467 loss via evasion was ~15% of C export from North Sea estuaries. By contrast, CO_2 evasion from
468 the Pamunkey and Mattaponi was appreciably greater (by 3-fold) relative to the James. Our
469 pCO_2 concentrations for the Pamunkey were similar to those previously reported by Raymond et
470 al. (2000), whereas our air-water flux values were higher (~3 g C m^{-2} d^{-1} vs. ~0.7 g C m^{-2} d^{-1}).
471 Comparisons of CO_2 fluxes are complicated by uncertainty regarding atmospheric exchange
472 (Raymond and Cole 2001; Borges et al. 2004; Raymond et al. 2017; Ward et al. 2017).
473 Raymond et al. (2000) used what they considered a conservative exchange coefficient (1.1 m d^{-1}).
474 More recent studies have adopted higher exchange coefficients, particularly for systems
475 where tidal and fluvial forces likely play a greater role in determining boundary layer conditions
476 than are predicted from wind-based models. Wind speeds are low in the upper segments of these
477 estuaries because the prevailing winds (SSW) are nearly perpendicular to the long axis of the
478 channel, which runs mostly east-west. Turbulence generated by strong tidal forces in shallow
479 channels likely plays a greater role in influencing boundary conditions for gas exchange
480 (Raymond and Cole 2001; Borges et al. 2004). These conditions support the use of higher
481 exchange coefficients than would be derived from wind speed alone.

482 Tidal fluxes were not a large component of the mass balance for any of the C fractions.
483 Although the volume of water exchanged during a tidal cycle was large (tidal prism = 28% of
484 estuarine volume), the elongate shape of the estuary dictates that water leaving on an out-going
485 tide returns on the subsequent in-coming tide. Results from the Cl mass balance suggest that the
486 net tidal exchange was ~7% of the tidal prism, equivalent to 2% of estuarine volume. In

addition, weak C gradients across the lower boundary of the study reach indicate that tidal inputs and outputs largely offset.

4.3 Metabolism & Carbon

Mass balance and metabolism data provide independent evidence that these estuaries are net heterotrophic. The mass balance indicates that the James is a sink for organic C and a source of inorganic C, consistent with metabolism data showing that ecosystem respiration exceeds GPP. Greater heterotrophy was observed in the Pamunkey where respiration rates were comparable to the James, but GPP was substantially lower. This finding was consistent with the observed higher CO_2 concentrations and efflux. The evasion of CO_2 from the Pamunkey and Mattaponi was large (3x) in comparison to riverine inputs of DOC and POC, whereas CO_2 loss from the James was ~50% of riverine OM inputs. Greater heterotrophy of the former is attributed to differences in hydrogeomorphology and forms of primary production. Higher chlorophyll-a values in the James indicate greater phytoplankton contributions to GPP, which brings the tidal fresh segment more closely in balance with respect to production and respiration. The Pamunkey and Mattaponi have low chlorophyll-a by comparison (Bukaveckas et al. 2020) but extensive lateral floodplains and emergent marshes (Hupp et al. 2009; Noe and Hupp 2009; Lake et al. 2013). Decomposition of terrestrial organic matter during floodplain inundation may account for the high CO_2 concentrations and air-water fluxes during high discharge conditions. Van Dam et al. (2018) similarly reported that high CO_2 losses during flooding events accounted for 30-40% of annual emissions from North Carolina estuaries. An accounting of changes in floodplain C stores before and after inundation events is needed to better understand their role in supporting respiration in these systems. Organic matter inputs following senescence of emergent vegetation may also contribute to higher rates of respiration and CO_2 evasion. Emergent plant production would not be captured in the diel dissolved-O_2 based estimates of ecosystem GPP, which may over-estimate heterotrophy in this system. Overall, C mass balance and ecosystem metabolism data show that the upper segments of these estuaries are net heterotrophic. This finding is consistent with a meta-analysis of metabolism data showing that estuaries are generally net heterotrophic (Hoellein et al. 2013), but contrasts with recent work by Brodeur et al. (2019) showing that the Susquehanna River and mainstem Chesapeake Bay are a net sink for DIC, and therefore net autotrophic. In the case of Chesapeake Bay, it may be that much of the

517 terrestrial organic matter (or at least, the POC fraction) is captured in the tributaries, thereby
518 favoring a prevalence of autochthony over allochthony, and GPP in excess of R.

519 Despite the large riverine influence in these upper estuarine segments, internal cycling of C via
520 production and respiration was large in comparison to external forcing via fluvial and tidal
521 exchange (Figure 11). In summer, remineralization of C via respiration was almost 2-fold
522 greater in comparison to external DIC inputs. In winter, the balance tipped strongly in favor of
523 external inputs as riverine DIC contributions were 3-fold greater than internal production via
524 respiration. Internal production of POC via GPP was an order of magnitude higher than external
525 inputs of POC in summer. In winter, GPP contributions were approximately equal to external
526 inputs of POC. Based on GPP, the estimated turnover time of the POC pool was 1.5 d in
527 summer. Taking into account that 60% of POC in the James is algal (Wood et al. 2016), the
528 estimated phytoplankton turnover time was 0.9 d. The high rates of internal biological
529 processing relative to through-puts of C places the James toward the lake-end, rather than the
530 stream-river end, on the metabolism and residence time spectrum (Hotchkiss et al. 2018). This is
531 likely a consequence of tidal conditions, which allow for longer water residence time compared
532 to non-tidal rivers. Proximal nutrient inputs (from riverine and point sources) and poor water
533 clarity (due to suspended sediments), likely also contribute to the dominance of phytoplankton
534 over aquatic plants in this system. If recent increases in water clarity continue (Henderson and
535 Bukaveckas 2021), we would expect a shift toward macrophyte dominance, lower GPP:ER, and
536 a diminished influence of internal C cycling.

537 The tidal fresh segment of the James has moderately low DIC and high GPP, which raises the
538 question whether primary production is limited by the availability of inorganic C. Our data show
539 that daily autotrophic C demand is small (~10%) relative to the available DIC pool. In summer,
540 DIC requirements to sustain GPP exceed the rate of external supply via river inputs, but
541 remineralization of C via respiration is approximately equal to GPP, indicating that internal
542 cycling is sufficiently large to preclude C limitation. However, a case could be made for
543 potential C limitation of photosynthesis due to depletion of pCO2. The diffusion of CO_2 in water
544 occurs more slowly than in air, potentially resulting in depletion during periods of high
545 autotrophic demand. In the James, low CO_2, with occasional under-saturation, was observed in
546 summer at stations corresponding to the CHLa maximum. Other studies in riverine settings have

shown that phytoplankton can reduce CO_2 to near or below atmospheric equilibrium (Raymond et al. 1997; Crawford et al. 2017). As CO_2 is energetically favored for carbon fixation, depletion of CO_2 may reduce production efficiency and alter community structure by favoring taxa capable of using bicarbonates. A number of prior studies have linked primary production and pCO2 (Jansson et al. 2012; Low-Decarie et al. 2015; Hasler et al. 2016). Our CO_2 data were collected mid-morning, closer to the diel maximum than the afternoon minimum (Crosswell et al. 2017; Reiman and Xu 2019), thereby potentially under-estimating CO_2 depletion. The possibility that phytoplankton-driven CO_2 depletion in the James may affect production and community composition cannot be discounted, though this effect appears limited to mid-summer and stations located at the CHLa maximum.

4.4 C Sources & Consumer Energetics

Lastly, I consider the utility of our C mass balance for understanding trophic energetics of the James food web, particularly with respect to autochthony and allochthony. Combining mass balance, ecosystem metabolism and bioenergetics is a potentially powerful approach to advancing our understanding of C cycles, but there are few examples, often, as in this case, due to a lack of data on consumer production (Ruegg et al. 2021). From a mass flux perspective, a comparison of autochthonous (GPP = 719 ± 32 g C m^{-2} y^{-1}) and allochthonous (POC= 298 ± 56, DOC = 340 ± 44 g C m^{-2} y^{-1}) inputs suggests that internal C sources are nearly equal (54 ± 4%) to external inputs, despite the large riverine influence in the upper estuary. These estimates can be refined to better reflect availability for consumers by discounting GPP by 40% to reflect loss via autotrophic respiration (Ruegg et al. 2021) and taking into account the fraction of POC and DOC that is retained (28 ± 3%). By this estimate, autochthonous production contributes 70% (431 g C m^{-2} y^{-1}) and allochthonous inputs 30% (203 g C m^{-2} y^{-1}) of C available to consumers. These percentages are based on annualized values though their relative importance varies seasonally with the majority of GPP occurring in May to October, and the bulk of POC delivered in January to May.

Comparisons of mass fluxes may not be indicative of C supporting secondary production if consumers preferentially utilize one source over another. A number of studies have suggested that autochthonous sources account for a disproportionately large fraction of C assimilation due to the higher nutritional quality of algae over partially decomposed terrestrial plant matter (Brett

et al. 2009; Thorp and Bowes 2017). Stable isotope analysis of the James food web has shown that the dominant metazoans by biomass, which are benthic omnivores (catfish, adult gizzard shad), carry a predominantly terrestrial C signature, whereas zooplankton and planktivorous fish (juvenile gizzard shad and threadfin shad) were dependent on autochthonous C sources (Wood et al. 2016). These patterns were consistent with analysis of basal resources showing that the sediments in the estuary were largely (90%) comprised of terrestrial C, whereas seston contained a greater fraction of autochthonous C (60% in summer).

The lack of secondary production data does not allow us to align C supply from autochthonous and allochthonous sources with C demands of consumers. However, the rate of biomass removal for one of the dominant metazoans (catfish) can be used as a first approximation of their annual production. Catfish were introduced to the James during the 1970's and 1980's and now dominate the fishery (Fabrizio et al. 2018), which has led to questions about their influence on food webs and ecosystem processes (Greenlee and Lim 2011; Hilling et al. 2019; Schmitt et al. 2019). The biomass of catfish removed from the James represents a conservative estimate of their annual production in that current harvest rates have not brought about declines in the catfish population, indicating that annual production exceeds the amount of biomass removed (Orth et al. 2017). During 2010-2020, the commercial harvest of catfish in the tidal James averaged 1,000,000 lbs y^{-1} (data provided by Virginia Marine Resources Commission), which taking into account the area of the fresh-brackish estuary, yields a harvest rate of 8.6 kg ha^{-1} y^{-1}. In addition to the commercial harvest, piscivorous birds are an important component of biomass removal. Here we focus on predation by bald eagles and osprey as there are census data during the breeding season (from areal surveys) and estimates of catfish contributions to adult and nestling diets (from direct observations and stable isotopes; Garman et al. 2010). Based on census data and bioenergetics modeling, fish consumption by bald eagles and osprey was estimated at 0.6 kg ha^{-1} d^{-1} for the James tidal fresh segment. Taking into account the contribution of catfish to the diet of bald eagles and osprey (~35%) yields an estimate of catfish biomass removal of 77 kg ha^{-1} y^{-1}, which is ~9-fold higher than for commercial fisheries. With further corrections for the moisture content (75%; Cresson et al. 2017) and C content of fish tissues (45%; Tanner et al. 2000), the total catfish removal by birds and commercial fishing is 0.96 g C m^{-2} y^{-1}. Their trophic position in the James (trophic level = 3.1; Orth et al. 2017) suggests a production efficiency of ~1% (Ruegg et al. 2021), which yields an estimated C demand to maintain this

level of production/harvest of 96 g C m^{-2} y^{-1}. The C demand for this introduced species corresponds to 15% of C available to consumers from allochthonous and autochthonous sources. Stable isotope data indicate that catfish in the James tidal fresh obtain 9% of their C from autochthonous sources and 81% from allochthonous sources (Wood et al. 2016). Applying these values suggests that 2% of GPP and 41% of allochthonous inputs are required to sustain current levels of catfish biomass removal from the James tidal fresh. The high rate of utilization for allochthonous inputs is consistent with our prior finding that consumer-mediated recycling is an important component of nutrient supply, and may account for the lack of response in primary production to large reductions in point source nutrient inputs (Wood et al. 2014).

4.5 Summary

Relatively complete C budgets are relatively rare, in part due to the effort involved in quantifying C fluxes from various sources (Hanson et al. 2015). This paper provides an accounting of C fluxes at the river-estuarine transition for three tributaries of Chesapeake over a span of years and discharge conditions. The findings show that the relative importance of external (river inputs & tidal exchange) vs. internal (metabolism) drivers differed among the three estuaries based on their physiographic setting and forms of primary production. Estuarine C forms were influenced by variable contributions from upland (DIC-rich, POC-rich) and lowland (DOC-rich) sources. Peak organic matter retention was associated with trapping of POC during high discharge conditions. Tidal exchange was not an important component of the C budget, whereas biological transformations via production and respiration were large in the phytoplankton-dominated James Estuary. Contrary to expectations, autochthonous sources accounted for the bulk of organic matter inputs despite the large riverine influence on the upper estuary. Commercial harvest data and previously derived estimates of piscivory by birds provided a basis for estimating consumer C demand, albeit for a single dominant species, and at a coarse (annualized) scale. Further progress in aligning C flows to food web energetics depends on the availability of production data for a greater range of consumers and at shorter time intervals. Bringing together C mass balance, ecosystem metabolism and consumer production data would enable a potentially powerful approach for advancing our understanding of how the timing and sources of C inputs constrain trophic energetics.

638 Acknowledgements

639 Thanks to Samantha Rogers who drafted figures for this paper, to D. Hopler, S. Tassone and W.
640 M. Lee who carried out the field and lab work, and to Donald Orth for helpful discussions
641 regarding catfish in the James. I am grateful to the USGS for providing discharge, DOC and
642 POC data for Fall Line stations and to the Virginia Institute of Marine Science for making
643 available dissolved oxygen data from the Pamunkey. This paper is dedicated to Jon Cole in
644 appreciation for his ability to turn numbers into interesting stories.

645 Data availability

646 Data can be accessed upon request to the corresponding author.

647 Competing interests

648 The author declares that there is no conflict of interest.

649

650 Reference List

651

652 Alin, S. R., F. L. de Fatima, M. Rasera, C. I. Salimon, J. E. Richey, G. W. Holtgrieve, A. V.
653 Krusche, and A. Snidvongs 2011. Physical controls on carbon dioxide transfer velocity
654 and flux in low-gradient river systems and implications for regional carbon budgets.
655 Journal of Geophysical Research: Biogeosciences 116: G01009.

656 Amann, T., A. Weiss, and J. Hartmann. 2012. Carbon dynamics in the freshwater part of the
657 Elebe estuary, Germany: Implications of improving water quality. Estuarine, Coastal and
658 Shelf Science 107: 112-121.

659 Amann, T., A. Weiss, and J. Hartmann. 2015. Inorganic carbon fluxes in the inner Elbe Estuary,
660 Germany. Estuaries and Coasts 38: 192-210.

661 Basu, B. K., and F. R. Pick 1996. Factors regulating phytoplankton and zooplankton biomass in
662 temperate rivers. Limnology and Oceanography 41: 1572-1577.

663 Bianchi, T. S. 2011. The role of terrestrially derived organic carbon in the coastal ocean: a
664 changing paradigm and the priming effect. Proceedings of the National Academy of
665 Sciences USA 108: 19473-19481.

666 Borges, A. V., B. Delille, L.-S. Schiettecatte, F. Gazeau, G. Abril, and M. Frankignoulle 2004.
667 Gas transfer velocities of CO2 in three European estuaries (Randers Fjord, Scheldt, and
668 Thames). Limnology and Oceanography 49: 1630-1641.

669 Brett, M. T., M. Kainz, S. Taipale, and H. Seshan 2009. Phytoplankton, not allochthonous
670 carbon, sustains herbivorous zooplankton production. Proceedings of the National
671 Academy of Sciences USA 106: 21197-21201.

672 Brodeur, J. R., B. Chen, J. Su, Y.-Y. Xu, N. Hussain, K. M. Scaboo, Y. Zhang, J. M. Testa, and
673 W.-J. Cai 2019. Chesapeake Bay inorganic carbon: distribution and seasonal variability.
674 Frontiers in Marine Science 6: 99.

675 Bukaveckas, P. A., L. E. Barry, M. J. Beckwith, V. David, and B. Lederer 2011. Factors
676 determining the location of the chlorophyll maximum and the fate of algal production
677 within the tidal freshwater James River. Estuaries and Coasts 34: 569-582.

678 Bukaveckas, P. A., and W. N. Isenberg. 2013. Loading, transformation and retention of nitrogen
679 and phosphorus in the tidal freshwater James River (Virginia). Estuaries and Coasts 36:
680 1219-1236.

681 Bukaveckas, P. A., and J. D. Wood 2014. Nitrogen retention in a restored tidal stream (Kimages
682 Creek, VA) assessed by mass balance and tracer approaches. Journal of Environmental
683 Quality 43: 1614-1623.

684 Bukaveckas, P. A., M. Beck, D. Devore, and W. M. Lee 2018. Climate variability and its role in
685 regulating C, N and P retention in the James River Estuary. Estuarine, Coastal and Shelf
686 Science 205: 161-173.

687 Bukaveckas, P. A., M. Katarzyte, A. Schlegel, R. Spuriene, T. A. Egerton, and D. Vaiciute 2019.
688 Composition and settling properties of suspended particulate matter in estuaries of the
689 Chesapeake Bay and Baltic Sea regions. Journal of Soils and Sediments 19: 2580-2593.

690 Bukaveckas, P. A., S. Tassone, W. M. Lee, and R. B. Franklin 2020. The influence of storm
691 events on metabolism and water quality of riverine and estuarine segments of the James,
692 Mattaponi and Pamunkey Rivers. Estuaries and Coasts 43: 1585-1602.

693 Butman, D., S. Stackpoole, E. G. Stets, C. P. McDonald, D. W. Clow, and R. G. Striegl 2016.
694 Aquatic carbon cycling in the conterminous United States and implications for terrestrial
695 carbon accounting. Proceedings of the National Academy of Sciences USA 113: 58-63.

696 Caffrey, J. M. 2003. Production, respiration and net ecosystem metabolism in U.S. estuaries.
697 Environmental Monitoring and Assessment 81: 207-219.

698 Caffrey, J. M. 2004. Factors controlling net ecosystem metabolism in U.S. estuaries. Estuaries
699 27: 90-101.

700 Cai, W.-J., and Y. Wang 1998. The chemistry, fluxes and sources of carbon dioxide in the
701 estuarine waters of the Satilla and Altamaha Rivers, Georgia. Limnology and
702 Oceanography 43: 657-668.

703 Cole, J. J., Y. T. Prairie, N. F. Caraco, W. H. McDowell, L. J. Tranvik, R. G. Striegl, C. M.
704 Duarte, P. Kortelainen, J. A. Downing, J. J. Middelburg, and J. M. Melack 2007.
705 Plumbing the global carbon cycle: integrating inland waters into the terrestrial carbon
706 budget. Ecosystems 10: 171-184.

707 Crawford, J. T., D. Butman, L. C. Loken, P. Stadler, C. Kuhn, and R. G. Striegl 2017. Spatial
708 variability of CO2 concentrations and biogeochemistry in the Lower Columbia River.
709 Inland Waters 7: 417-427.

710 Cresson, P., M. Travers-Trolet, M. Rouquette, C-A. Timmerman, C. Giraldo, S. Lefebvre, and B.
711 Ernande. 2017. Underestimation of chemical contamination in marine fish muscle tissue
712 can be reduced by considering variable wet:dry weight ratios. Marine Pollution Bulletin.
713 123: 279-285.

714 Crosswell, J. R., I. C. Anderson, J. W. Stanhope, B. Van Dam, M. J. Brush, S. H. Ensign, M. F.
715 Piehler, B. McKee, M. Bost, and H. W. Paerl 2017. Carbon budget of a shallow lagoonal
716 estuary: transformations and source-sink dynamics along the river-estuary-ocean
717 continuum. Limnology and Oceanography 62: S29-S45.

718 Fabrizio, M. C., T. D. Tuckey, R. J. Latour, G. C. White, and A. J. Norris 2018. Tidal habitats
719 support large numbers of invasive blue catfish in a Chesapeake Bay sub-estuary.
720 Estuaries and Coasts 41: 827-840.

721 Garman, G., C. Viverette, B. Watts, and S. Macko. 2010. Predator-prey Interactions among
722 Fish-eating Birds and selected Fishery Resources in the Chesapeake Bay: Temporal and
723 Spatial Trends and Implications for Fishery Assessment and Management. William &
724 Mary Center for Conservation Biology Technical Report #349.
725 https://scholarworks.wm.edu/ccb_reports/349.

726 Gellis, A.C. and others. 2009. Sources, transport, and storage of sediment in the Chesapeake
727 Bay Watershed. U.S. Geological Survey Scientific Investigations Report 2008–5186.

728 Greenlee, R. S., and C. N. Lim 2011. Searching for equilibrium: population parameters and
729 variable recruitment in introduced blue catfish populations in four Virginia tidal river
730 systems. American Fisheries Society Symposium 77: 349-367.

731 Hanson, P. C., M. L. Pace, S. R. Carpenter, J. J. Cole, and E. H. Stanley 2015. Integrating
732 landscape carbon cycling: research needs for resolving organic carbon budgets of lakes.
733 Ecosystems 18: 363-375.

734 Hasler, C. T., D. Butman, J. D. Jeffrey, and C. D. Suski 2016. Freshwater biota and rising pCO2?
735 Ecology Letters 19: 98-108.

736 Henderson, R. and P.A. Bukaveckas. 2021. Factors governing light attenuation in upper
737 segments of the James and York Estuaries and their influence on primary producers.
738 Estuaries & Coasts https://doi.org/10.1007/s12237-021-00983-6.

739 Hilling, C. D., A. J. Bunch, J. A. Emmel, J. D. Schmitt, and D. J. Orth 2019. Growth and
740 mortality of invasive flathead catfish in the tidal James River, Virginia. Journal of Fish
741 and Wildlife Management 10: 641-652.

742 Hoellein, T. J., D. A. Bruesewitz, and D. C. Richardson 2013. Revisiting Odum (1956): a
743 synthesis of aquatic ecosystem metabolism. Limnology and Oceanography 58: 2089-
744 2100.

745 Hoffman, J. C., D. A. Bronk, and J. E. Olney 2008. Organic matter sources supporting lower
746 food web production in the tidal freshwater portion of the York River estuary. Estuaries
747 and Coasts 31: 898-911.

748 Hotchkiss, E. R., S. Sadro, and P. C. Hanson 2018. Toward a more integrative perspective on
749 carbon metabolism across lentic and lotic inland waters. Limnology and Oceanography:
750 Letters 3: 57-63.

751 Hoitink, A. J. F., and D. A. Jay 2016. Tidal river dynamics: implications for deltas. Reviews of
752 Geophysics 54: 240-272.

753 Holgerson, M. A., and P. A. Raymond 2016. Large contribution to inland water CO_2 and CH_4
754 emissions from very small ponds. Nature Geoscience doi: 10.1038/ngeo2654.

755 Hupp, C. R., A. R. Pierce, and G. B. Noe 2009. Floodplain geomorphic processes and
756 environmental impacts of human alteration along Coastal Plain rivers, USA. Wetlands
757 29: 413-429.

758 Jansson, M., J. Karlsson, and A. Jonsson 2012. Carbon dioxide super-saturation promotes
759 primary production in lakes. Ecology Letters 15: 527-532.

760 Joesoef, A., D. L. Kirchman, C. K. Sommerfield, and W.-J. Cai 2017. Seasonal variability of the
761 inorganic carbon system in a large coastal plain estuary. Biogeosciences 14: 4949-4963.

762 Jones, A. E., B. R. Hodges, J. W. McClelland, A. K. Hardison, and K. B. Moffett 2017.
763 Residence-time-based classification of surface water systems. Water Resources Research
764 53: 5567-5584.

765 Jones, A. E., A. K. Hardison, B. R. Hodges, J. W. McClelland, and K. B. Moffett 2020. Defining
766 a riverine tidal freshwater zone and its spatiotemporal dynamics. Water Resources
767 Research 56: e2019WRR026619.

768 Lake, S.J., M.J. Brush, I.C. Anderson, and H.I. Kator. 2013. Internal versus external drivers of
769 periodic hypoxia in a coastal plain tributary estuary: the York River, Virginia. Marine
770 Ecology Progress Series 492: 21-39.

771 Lionard, M., K. Muylaert, A. Hanoutti, T. Maris, M. Tackx, and W. Vyverman 2008. Inter-
772 annual variability in phytoplankton summer blooms in the freshwater tidal reahes of the
773 Schelde estuary (Belgium). Estuarine, Coastal and Shelf Science 79: 694-700.

774 Low-Decarie, E., G. Bell, and G. F. Fussman 2015. CO2 alters community composition and
775 response to nutrient enrichment of freshwater phytoplankton. Oecologia 177: 875-883.

776 Lucas, L. V., J. K. Thompson, and L. R. Brown 2009. Why are diverse relationships observed
777 between phytoplankton biomass and transport time? Limnology and Oceanography 54:
778 381-390.

779 Meybeck, M. 2003. Global analyses of river systems: from Earth system controls to
780 Anthropocene syndromes. Phil. Trans. R. Soc. Lond. B 358: 1935-1955.

781 Middelburg, J. J., and P. M. J. Herman 2007. Organic matter processing in tidal estuaries. Marine
782 Chemistry 106: 127-147.

783 Morton, R., and B. L. Henderson 2008. Estimation of non-linear trends in water quality: an
784 improved approach using generalized additive models. Water Resources Research 44:
785 W07420.

786 Murphy, R. R., E. Perry, J. Harcum, and J. Keisman 2019. A Generalized Additive Model
787 approach to evaluating water quality: Chesapeake Bay case study. Environmental
788 Modelling and Software 118: 1-13.

789 Muylaert, K., M. Tackx, and W. Vyverman 2005. Phytoplankton growth rates in the tidal
790 freshwater reaches of the Schelde estuary (Belgium) estimated using a simple light-
791 limited primary production model. Hydrobiologia 540: 127-140.

792 Noe, G. B., and C. R. Hupp 2009. Retention of riverine sediment and nutrient loads by Coastal
793 Plain floodplains. Ecosystems 12: 728-746.

794 Orth, D.J., Y. Jiao, J.D. Schmidt, C.D. Hilling, J.A. Emmel and M.C. Fabrizio. 2017. Dynamics
795 and Role of Non-native Blue Catfish *Ictalurus furcatus* in Virginia's Tidal Waters. Final
796 Report submitted to Virginia Department of Game and Inland Fisheries. DOI:
797 10.13140/RG.2.2.35917.54246.

798 Pace, M. L., S. E. G. Findlay, and D. Lints 1992. Zooplankton in advective environments: the
799 Hudson River community and a comparative analyses. Canadian Journal of Fisheries and
800 Aquatic Sciences 49: 1060-1069.

801 Patrick, C. J., and others 2020. A system level analysis of coastal ecosystem responses to
802 hurricane impacts. Estuaries and Coasts 43: 943-959.

803 Qin, Q., and J. Shen 2017. The contribution of local and transport processes to phytoplankton
804 biomass variability over different time scales in the Upper James River, Virginia.
805 Estuarine, Coastal and Shelf Science 196: 123-133.

806 Raymond, P. A., J. E. Bauer, and J. J. Cole 2000. Atmospheric CO2 evasion, dissolved inorganic
807 carbon production, and net heterotrophy in the York River estuary. Limnology and
808 Oceanography 45: 1707-1717.

809 Raymond, P. A., N. F. Caraco, and J. J. Cole 1997. Carbon dioxide concentration and
810 atmospheric flux in the Hudson River. Estuaries 20: 381-390.

811 Raymond, P. A., and J. J. Cole 2001. Gas exchange in rivers and estuaries: Choosing a gas
812 transfer velocity. Estuaries 24: 312-317.

813 Raymond, P. A., J. Hartmann, R. Lauerwald, S. Sobek, C. P. McDonald, M. Hoover, D. Butman,
814 R. G. Striegl, E. Mayorga, C. Humborg, P. Kortelainen, H. Durr, M. Meybeck, P. Ciais,
815 and P. Guth 2017. Global carbon dioxide emissions from inland waters. Nature 503: 355-
816 359.

817 Reiman, J. H., and Y. J. Xu 2019. Diel variability of PCO2 and CO2 outgassing from the lower
818 Mississippi River: implications for riverine CO2 outgassing estimation. Water 11: 43.

819 Richey, J. E., J. M. Melack, A. Aufdenkampe, V. M. Ballester, and L. L. Hess 2002. Outgassing
820 from Amazonian rivers and wetlands as a large tropical source of atmospheric CO2.
821 Nature 416: 617-620.

822 Robson, B. J., P. A. Bukaveckas, and D. P. Hamilton 2008. Modelling and mass balance
823 assessments of nutrient retention in a seasonally-flowing estuary (Swan River Estuary,
824 Western Australia). Estuarine, Coastal and Shelf Science 76: 282-292.

825 Ruegg, J., C. C. Conn, E. P. Anderson, T. J. Battin, E. S. Bernhardt, M. B. Canadell, S. M.
826 Bonjour, J. D. Hosen, N. S. Marzolf, and C. B. Yackulic 2021. Thinking like a consumer:
827 linking aquatic basal metabolism and consumer dynamics. Limnology and
828 Oceanography: Letters 6: 1-17.

829 Schmitt, J. D., B. K. Peoples, L. Castello, and D. J. Orth 2019. Feeding ecology of generalist
830 consumers: a case study of invasive blue catfish Ictalurus furcatus in Chesapeake Bay,
831 Virginia, USA. Environmental Biology of Fishes 102: 443-465.

832 Sellers, T., and P. A. Bukaveckas 2003. Phytoplankton production in a large, regulated river: A
833 modeling and mass balance assessment. Limnology and Oceanography 48: 1476-1487.

834 Shen, J., and J. Lin 2006. Modeling study of the influences of tide and stratification on age of
835 water in the tidal James River. Estuarine, Coastal and Shelf Science 68: 101-112.

836 Soballe, D. M., and B. L. Kimmel 1987. A large-scale comparison of factors influencing
837 phytoplankton abundance in rivers, lakes, and impoundments. Ecology 68: 1943-1954.

838 Steen, A.D., L. M. Quigley and A. Buchan. 2015. Evidence for the priming effect in a
839 planktonic estuarine microbial community. Frontiers in Marine Science 3:6.
840 doi:10.3389/fmars.2016.00006.

841 Tassone, S., and P. A. Bukaveckas 2019. Seasonal, interannual and longitudinal patterns in
842 estuarine metabolism derived from diel oxygen data using multiple computational
843 approaches. Estuaries and Coasts 42: 1032-1051.

844 Thorp, J. H., and R. E. Bowes 2017. Carbon sources in riverine food webs: new evidence from
845 amino acid isotope techniques. Ecosystems 20: 1029-1041.

846 Tranvik, L. J., J. A. Downing, J. B. Cotner, and others 2009. Lakes and reservoirs as regulators
847 of carbon cycling and climate. Limnology and Oceanography 54: 2298-2314.

848 Tranvik, L. J., J. J. Cole, and Y. T. Prairie 2018. The study of carbon in inland waters - from
849 isolated ecosystems to players in the global carbon cycle. Limnology and Oceanography:
850 Letters 3: 41-48.

Van Dam, B. R., J. R. Crosswell, and H. W. Paerl 2018. Flood-driven CO2 emissions from adjacent North Carolina estuaries during Hurricane Joaquin (2015). Marine Chemistry 207: 1-12.

Vincent, W. F., J. J. Dodson, N. Bertrand, and J.-J. Frenette 1996. Photosynthetic and bacterial production gradients in a larval fish nursery: The St. Lawrence River transition zone. Marine Ecology Progress Series 139: 227-238.

Volta, C., G. G. Laruelle, and P. Regnier 2016. Regional carbon and CO2 budgets of North Sea tidal estuaries. Estuarine, Coastal and Shelf Science 176: 76-90.

Vorosmarty, C. J., M. Meybeck, B. M. Fekete, K. P. Sharma, P. Green, and J. P. M. Syvitski 2003. Anthropogenic sediment retention: major global impact from registered river impoundments. Global and Planetary Change 39: 169-190.

Ward, N. D. and others. 2016. The reactivity of plant-derived organic matter and the potential importance of priming effects in the lower Amazon River. JGR-Biogeosciences 121: 1522–1539.

Ward, N. D., T. S. Bianchi, P. M. Medeiros, M. Seidel, J. E. Richey, R. G. Keil, and H. O. Sawakuchi 2017. Where carbon goes when water flows: carbon cycling across the aquatic continuum. Frontiers in Marine Science 4: 7.

Wiik, E., H. A. Haig, N. M. Hayes, K. Finlay, G. L. Simpson, R. J. Vogt, and P. R. Leavitt 2021. Generalized additive models of climatic and metabolic controls of subannual variation in pCO2 in productive hardwater lakes. Journal of Geophysical Research: Biogeosciences 123: 1940-1959.

Wood, J. D., and P. A. Bukaveckas 2014. Increasing severity of phytoplankton nutrient limitation following reductions in point source inputs to the tidal freshwater segment of the James River Estuary. Estuaries and Coasts 37: 1188-1201.

Wood, J. D., D. Elliott, G. C. Garman, D. Hopler, W. Lee, S. McIninch, A. J. Porter, and P. A. Bukaveckas 2016. Autochthony, allochthony and the role of consumers in influencing the sensitivity of aquatic systems to nutrient enrichment. Food Webs 7: 1-12.

Wood, S., 2006. Generalized Additive Models: an Introduction with R, 1 ed. Chapman and Hall/CRC, Boca Raton, FL.

Wymore, A. S., H. M. Fazekas, and W. H. McDowell 2021. Quantifying the frequency of synchronous carbon and nitrogen export to the river network. Biogeochemistry 152: 1-12.

Xu, X., and others 2021. Tidal freshwater zones as hotspots for biogeochemical cycling: sediment organic matter decomposition in the lower reaches of two South Texas rivers. Estuaries and Coasts 44 : 722-733.

Yang, G., and D. L. Moyer 2020. Estimation of non-linear water quality trends in high-frequency monitoring data. Science of the Total Environment 715: 136686.

Young, M., E. Hoew, T. O'Rear, K. Berridge, and P. Moyle 2021. Food web fuel differs across habitats and seasons of a tidal freshwater estuary. Estuaries and Coasts 44: 286-301.

889 Zarnetske, J. P., M. Bouda, B. W. Abbott, J. Saiers, and P. A. Raymond 2018. Generality of
890 hydrologic transport limitation of watershed organic carbon flux across ecoregions of the
891 United States. Geophysical Research Letters 45: 11702-11711.

892 Table 1. Data collection sites for this study include USGS Fall Line gauging stations (Q denotes
893 discharge), estuarine sampling sites and an ungauged Coastal Plain tributary of the James
894 (Kimages Creek). Station numbers denote distance in river miles from the confluence with
895 Chesapeake Bay (James) or the York (Pamunkey and Mattaponi). Observations denote the
896 number of sampling dates for water chemistry within the specified time span.

Tributary	Segment	Stations	Parameters	Years	Observations	Source
James	River	JMS110	Q, DOC, POC	2010-19	197	USGS (02037500)
		JMS110	Cl, DIC, pCO_2	2012-19	189	This Study
	Estuary	JMS99,75,69,56	Cl, DOC, POC, DIC, pCO_2	2015-19	105	This Study
	Ungauged	Kimages Creek	Cl, DOC, POC, DIC, pCO2	2012-19	211	This Study
Pamunkey	River	PMK82	Q, DOC, POC	2010-19	202	USGS (01673000)
	Estuary	PMK50,39,6	DOC, POC, DIC, pCO_2	2017-19	60	This Study
Mattaponi	River	MPN54	Q, DOC, POC	2010-19	203	USGS (01674500)
	Estuary	MPN36,29,4	DOC, POC, DIC, pCO_2	2017-19	60	This Study

897

898

899 Table 2. GAM analysis of seasonal (day of year; DOY), inter-annual (date) and discharge
900 dependent variation in river, tributary and estuarine DOC, POC, DIC, pCO_2 and Cl. Data are for
901 riverine and upper estuarine segments of the James, Mattaponi and Pamunkey as well as a local
902 (below Fall Line) tributary (Kimages Creek). Statistics include the adjusted R^2, root mean
903 square error (RMSE as mg L^{-1}, except pCO_2 = ppmv), and significance of s values with their
904 effective degrees of freedom (** denotes $p < 0.001$; * $p < 0.05$).

905

Model	Fraction	Site	Adj R^2	RMSE	s(DOY)	s(date)	s(discharge)
River	DOC	James	0.50	0.82	3.42**	8.52**	3.00**
		Mattaponi	0.81	1.00	5.66**	8.93**	5.43**
		Pamunkey	0.67	1.06	4.64**	8.61**	5.54**
	POC	James	0.76	1.74	3.67**	7.89**	8.20**
		Mattaponi	0.38	0.61	3.99**	6.34	6.25**
		Pamunkey	0.51	1.08	2.39**	8.95**	7.79**
	DIC	James	0.44	4.19	2.42**	7.89**	8.20**
	pCO_2	James	0.67	149	3.37**	6.43**	3.59**
	Cl	James	0.48	4.36	7.23**	8.30**	6.73**
Tributary	DOC	Kimages	0.33	3.22	4.70**	8.26**	NA
	POC	Kimages	0.24	0.57	4.61**	7.63**	NA
	DIC	Kimages	0.19	3.00	0.41	8.26**	NA
	Cl	Kimages	0.23	8.63	6.46**	6.48**	NA
Estuary	DOC	James	0.13	3.44	4.29	1.96	1.91*
		Mattaponi	0.27	2.37	5.65	3.42**	1.00
		Pamunkey	0.27	2.61	5.94*	3.95**	1.00
	POC	James	0.75	0.22	5.77**	2.64**	3.68**
		Mattaponi	0.14	0.53	1.79*	1.00	4.13**
		Pamunkey	0.40	0.30	2.46**	1.27	7.59**
	DIC	James	0.76	1.55	1.27**	4.41**	2.50**
		Mattaponi	0.74	2.05	1.74**	2.27**	1.48**
		Pamunkey	0.68	2.10	1.30*	3.16**	1.00**
	pCO_2	James	0.40	241	5.84**	3.48	2.38*
		Mattaponi	0.82	367	3.31**	2.65**	4.14**
		Pamunkey	0.81	357	3.81**	2.73**	4.01**
	Cl	James	0.46	24.7	6.26**	8.54**	6.97**

906

907

Figure 1. Map showing USGS discharge gauging locations, estuarine sampling sites and continuous dissolved oxygen monitoring locations on the Mattaponi, Pamunkey and James. Inset: James and York watersheds in relation to physiographic provinces.

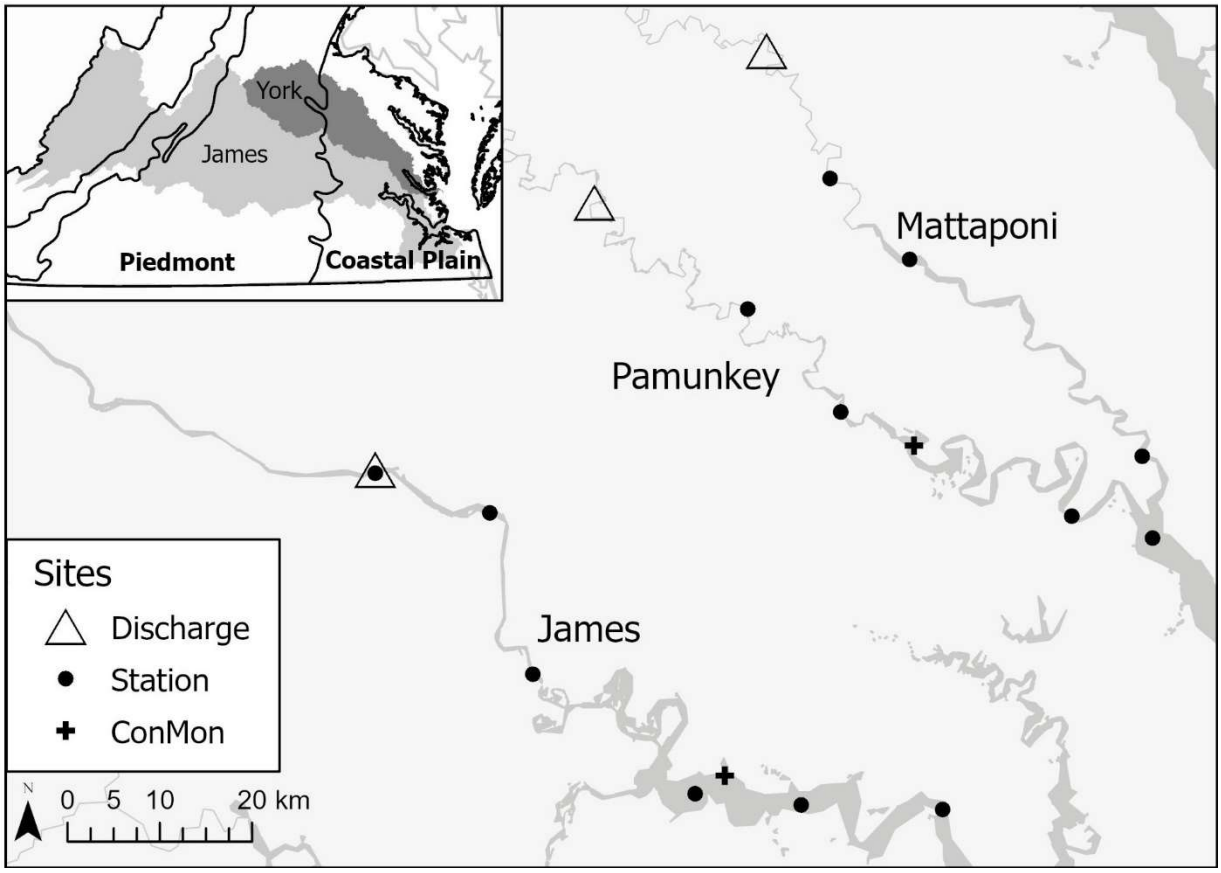

Figure 2. Seasonal variation in instantaneous discharge measured at the Fall Line of the James, Mattaponi and Pamunkey Rivers. Here and in subsequent figures, symbols denote median (bar), 25 and 75 %-tiles (box), 5 and 95 %-tiles (whiskers) and outliers (dots).

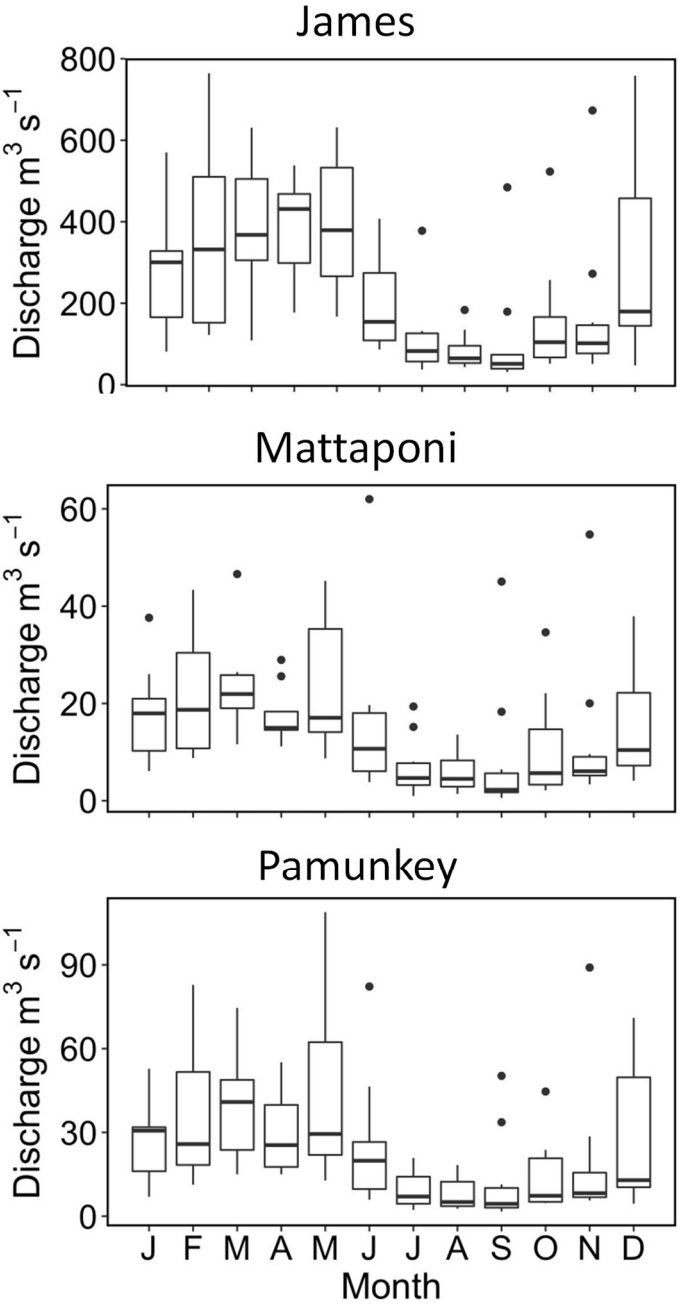

Figure 3. Time series of Cl concentrations in the tidal fresh segment of the James Estuary (upper panel) and Cl fluxes associated with river inputs, estuarine export and net tidal exchange (lower panels).

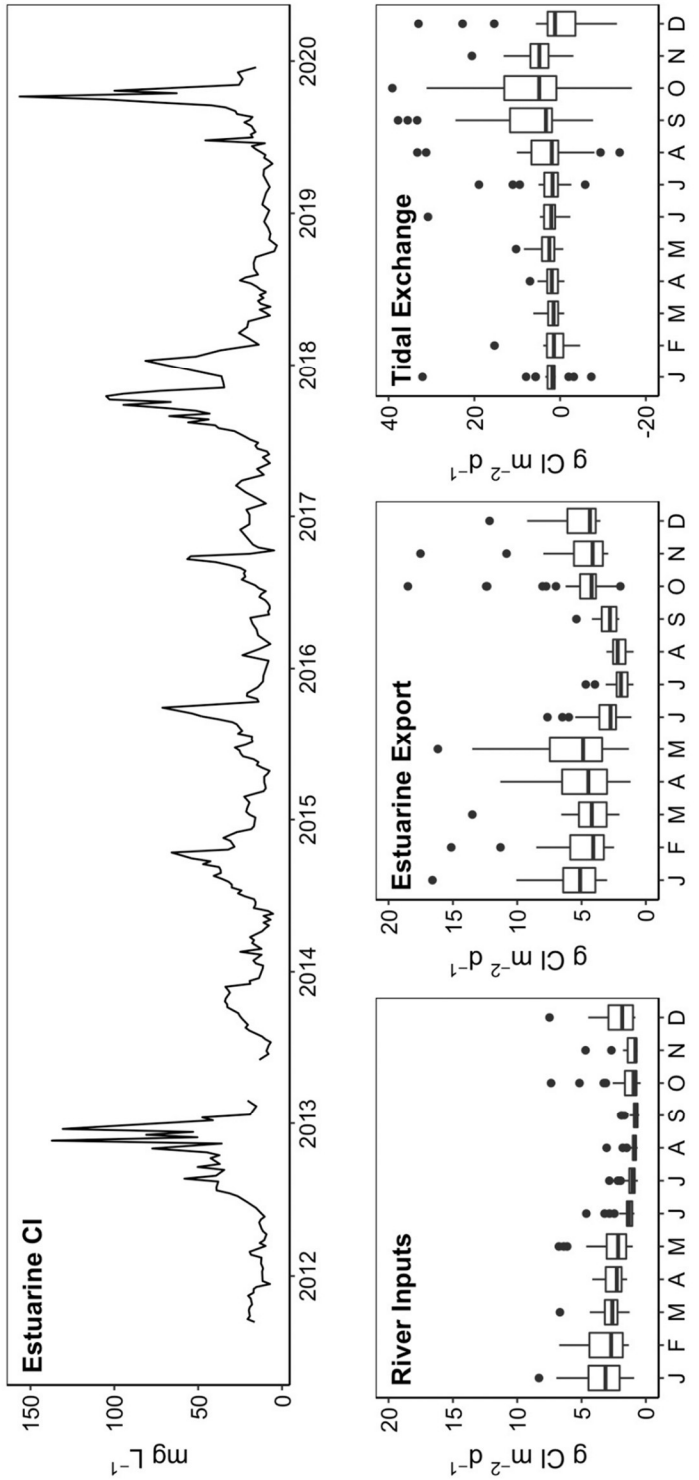

Figure 4. Results from GAM analysis depicting changes in riverine DOC, POC and DIC as a function of discharge (Q) for the James Mattaponi and Pamunkey Rivers.

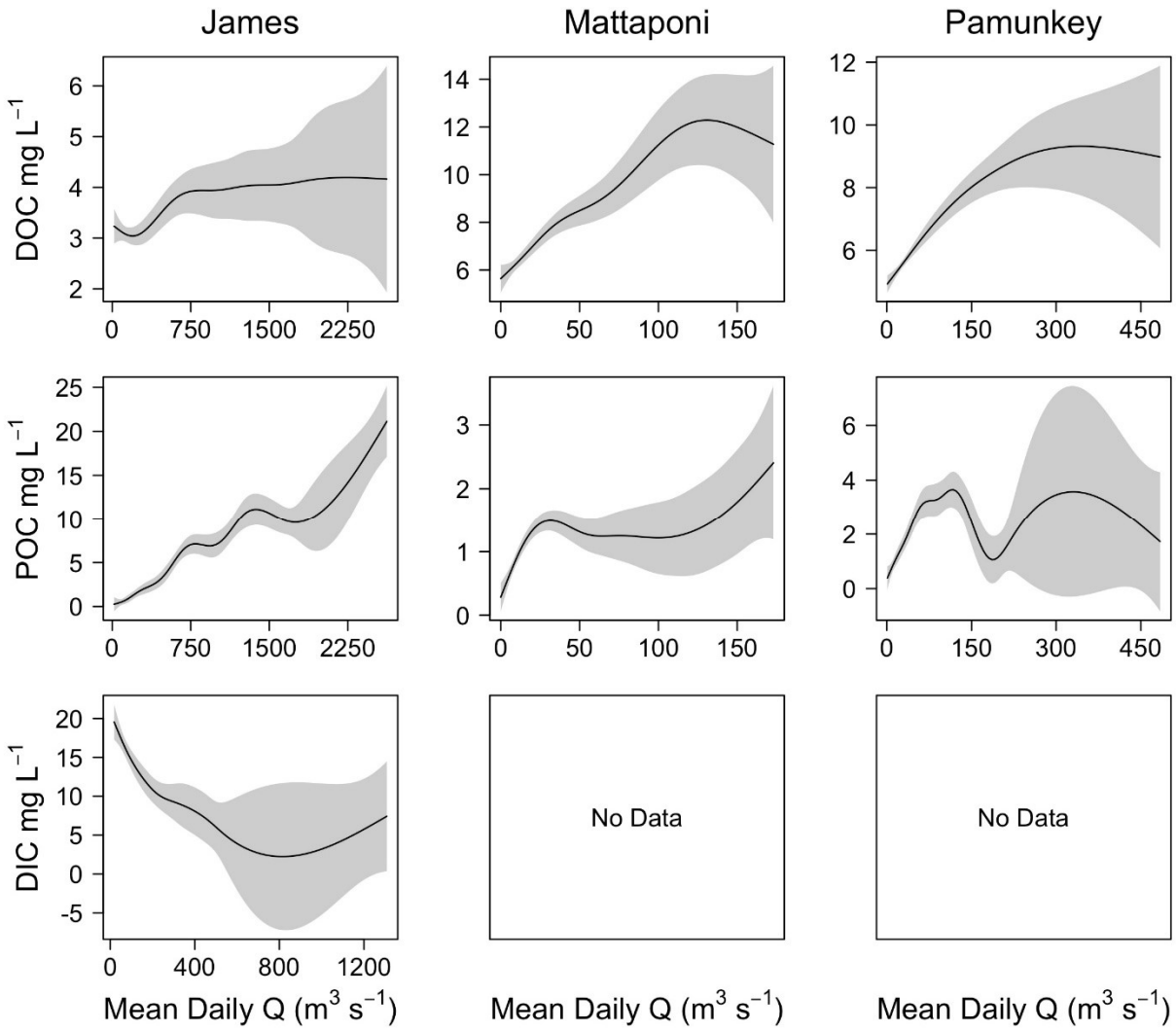

Figure 5. Results from GAM analysis depicting the effects of discharge (Q) on estuarine DOC, POC and DIC for the James Mattaponi and Pamunkey Estuaries. Concentrations are volume-weighted averages among estuarine sampling locations.

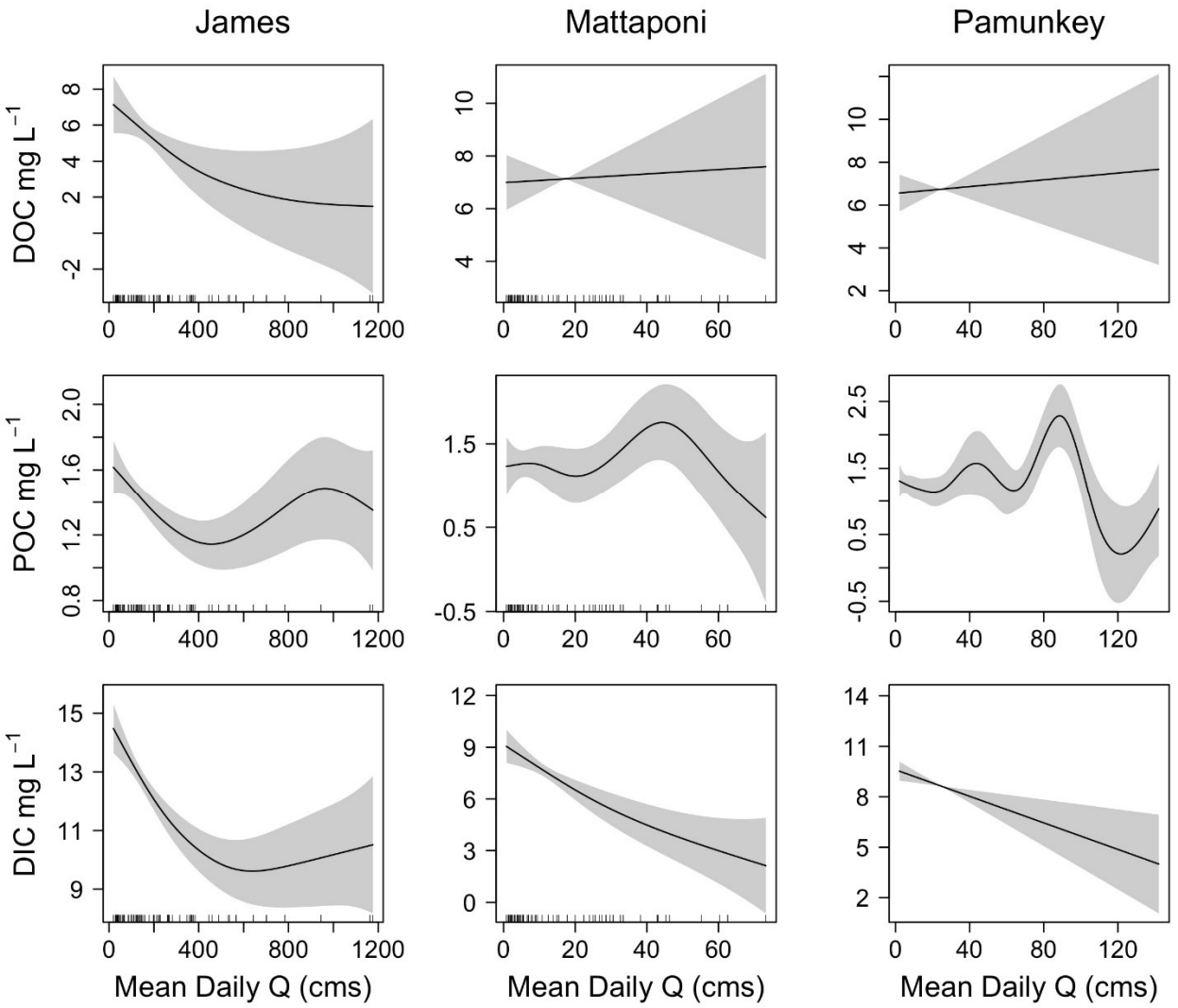

Figure 6. Results from GAM analysis depicting seasonal (day of year; DOY), inter-annual (decimal date) and discharge dependent variation in pCO_2 of the James, Mattaponi and Pamunkey Estuaries. Analyses were based on volume-weighted averages from 3-4 sampling locations in each estuary.

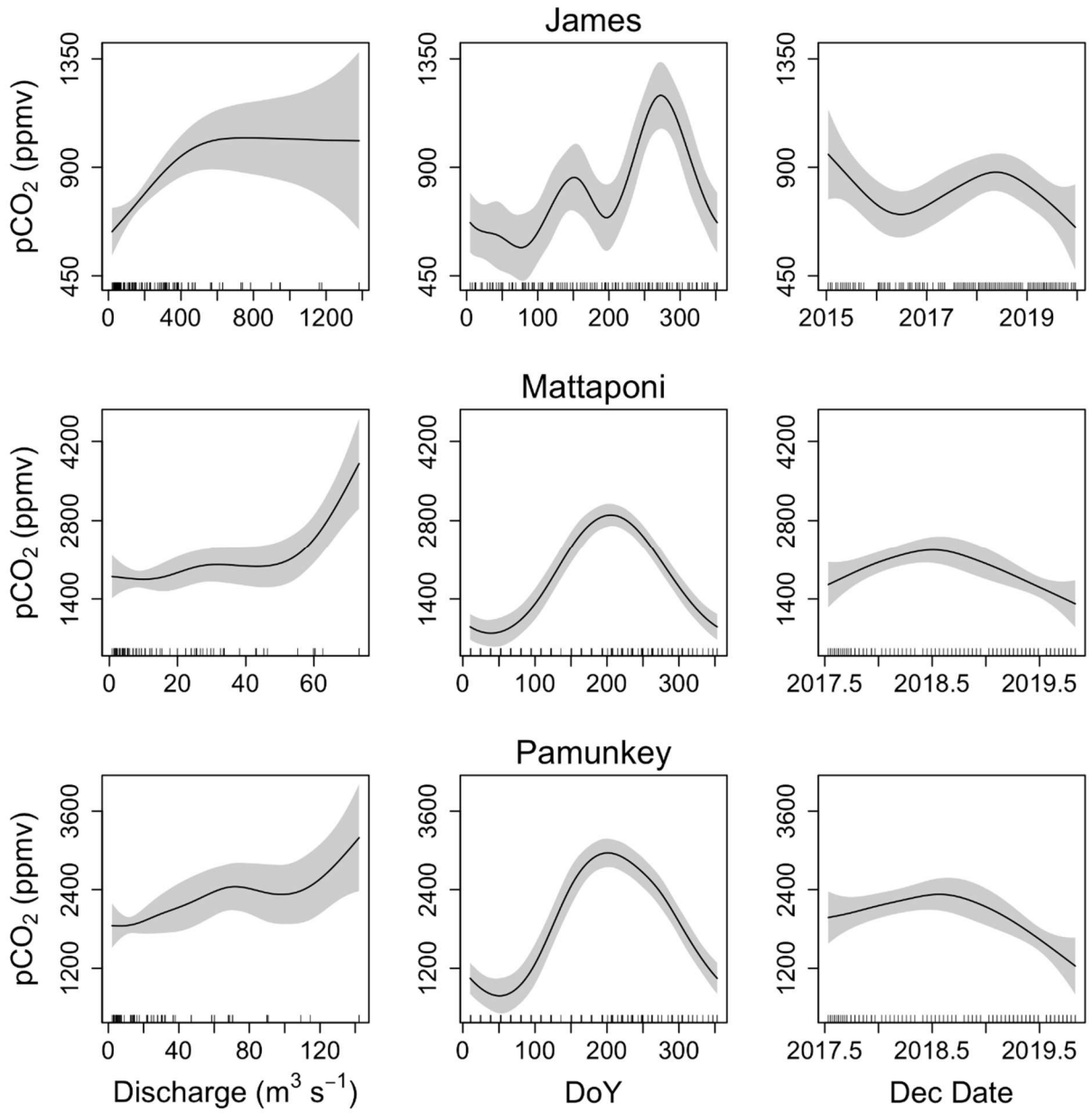

Figure 7. Monthly average values of air-water CO_2 fluxes for the James, Mattaponi and Pamunkey Estuaries. Positive values denote efflux of CO_2 from the estuary.

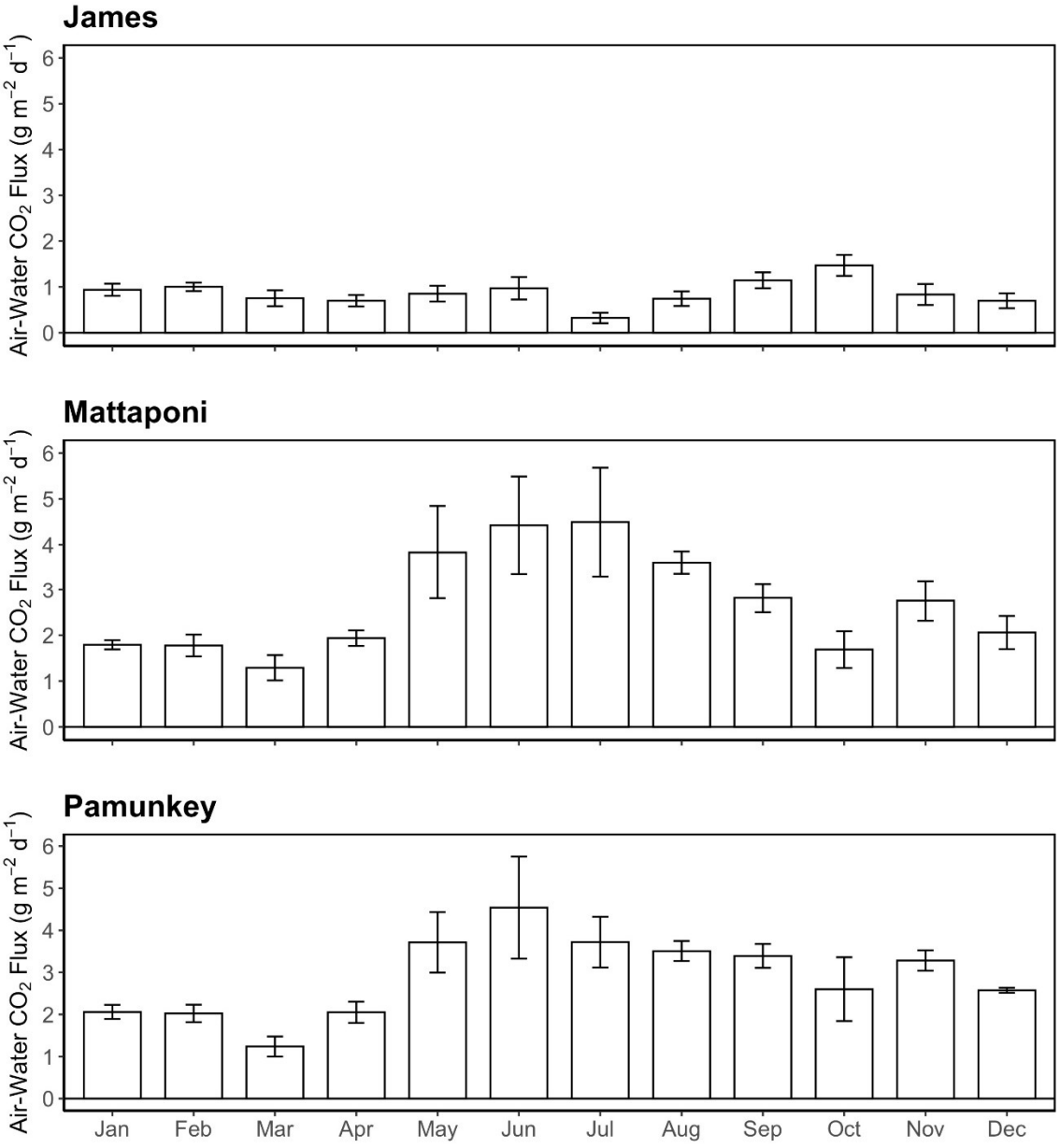

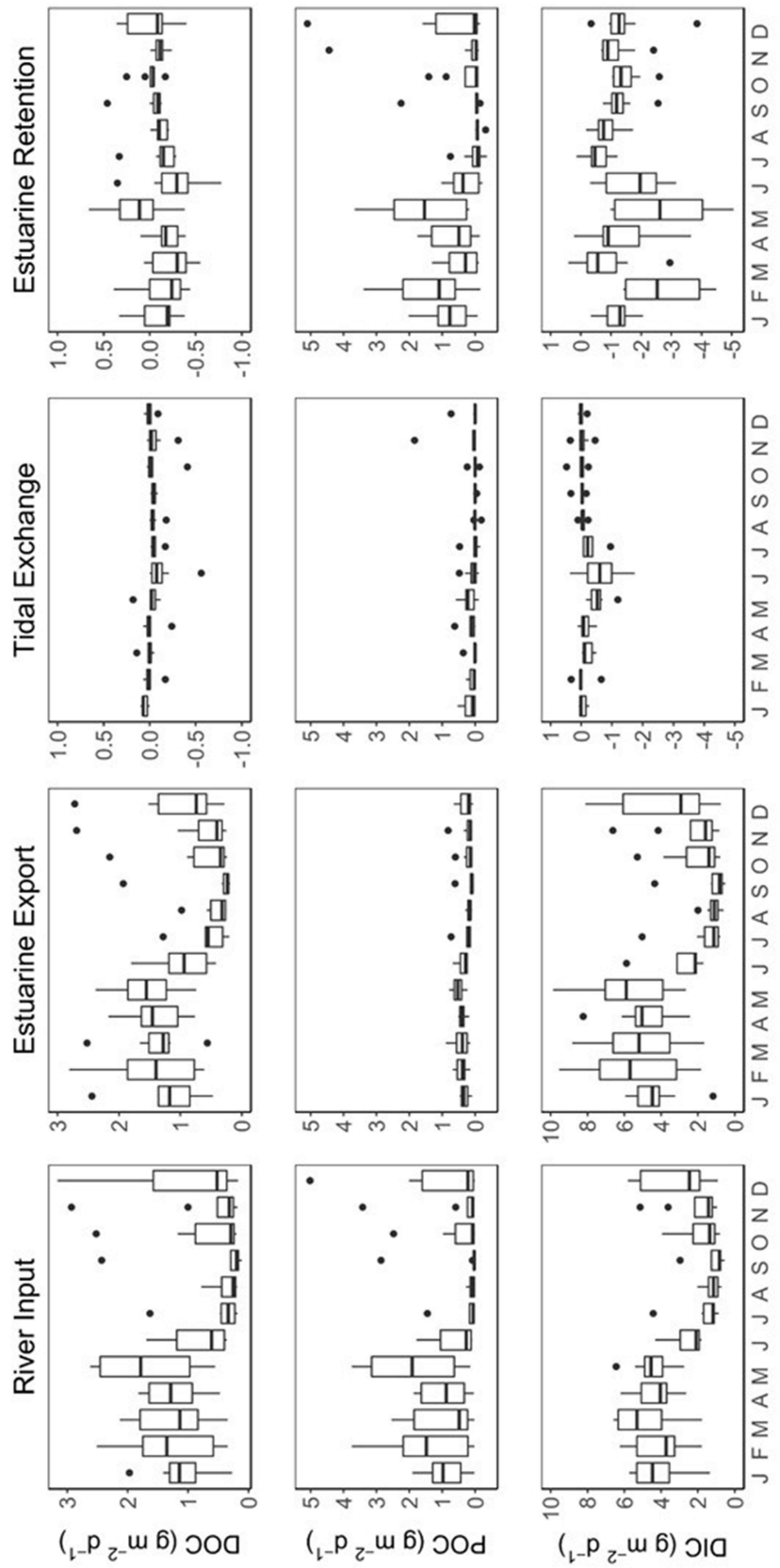

Figure 8. Seasonal variation in DOC, POC and DIC fluxes associated with riverine inputs, estuarine export, tidal exchange and estuarine retention for the tidal freshwater segment of the James Estuary (note differences in y axis scaling). Negative values for estuarine retention denote a net loss. DIC retention estimates take into account atmospheric losses of CO_2.

Figure 9. River input and estuarine export fluxes of DOC and POC for the Pamunkey (PMK) and Mattaponi (MPN) estuaries.

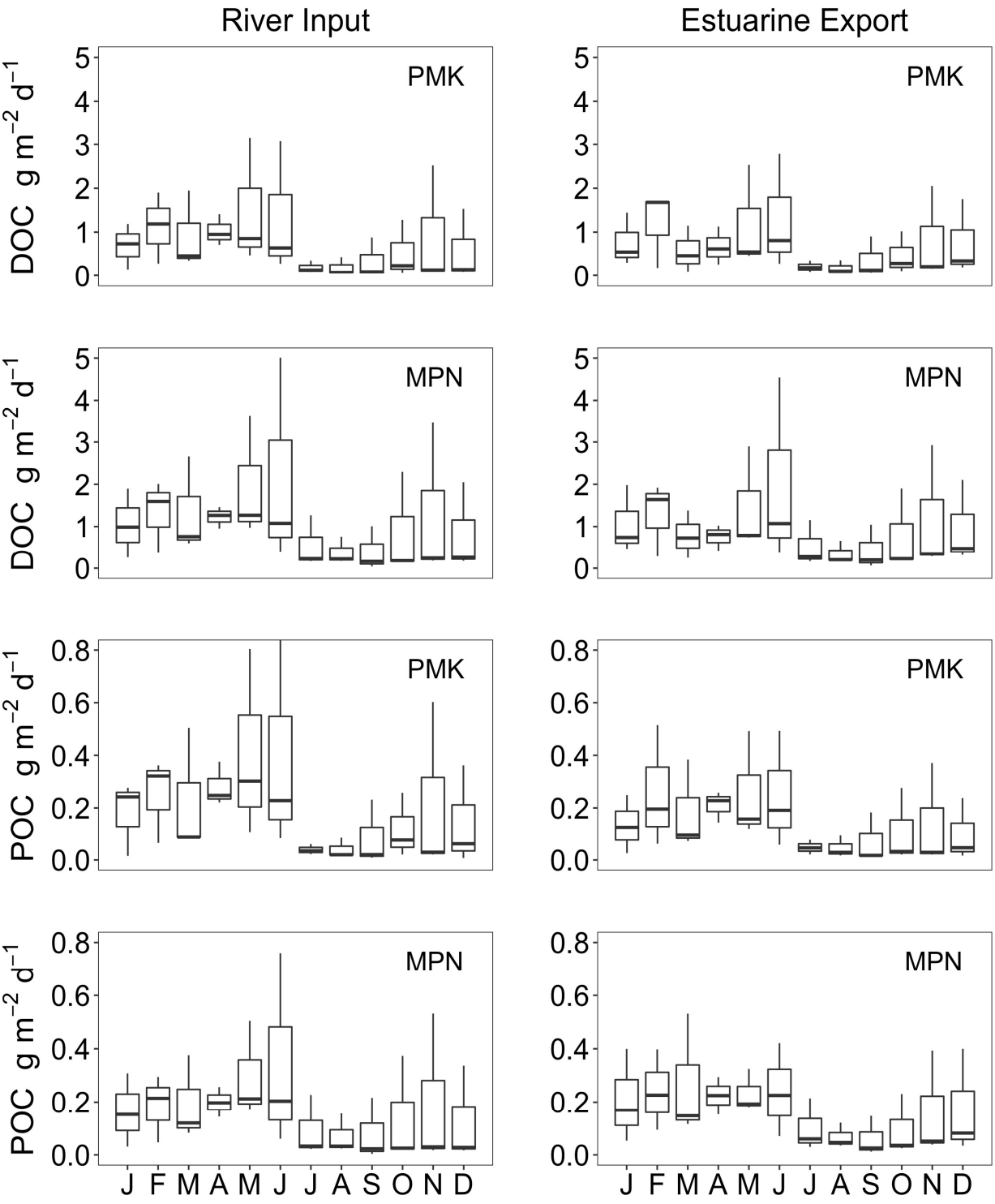

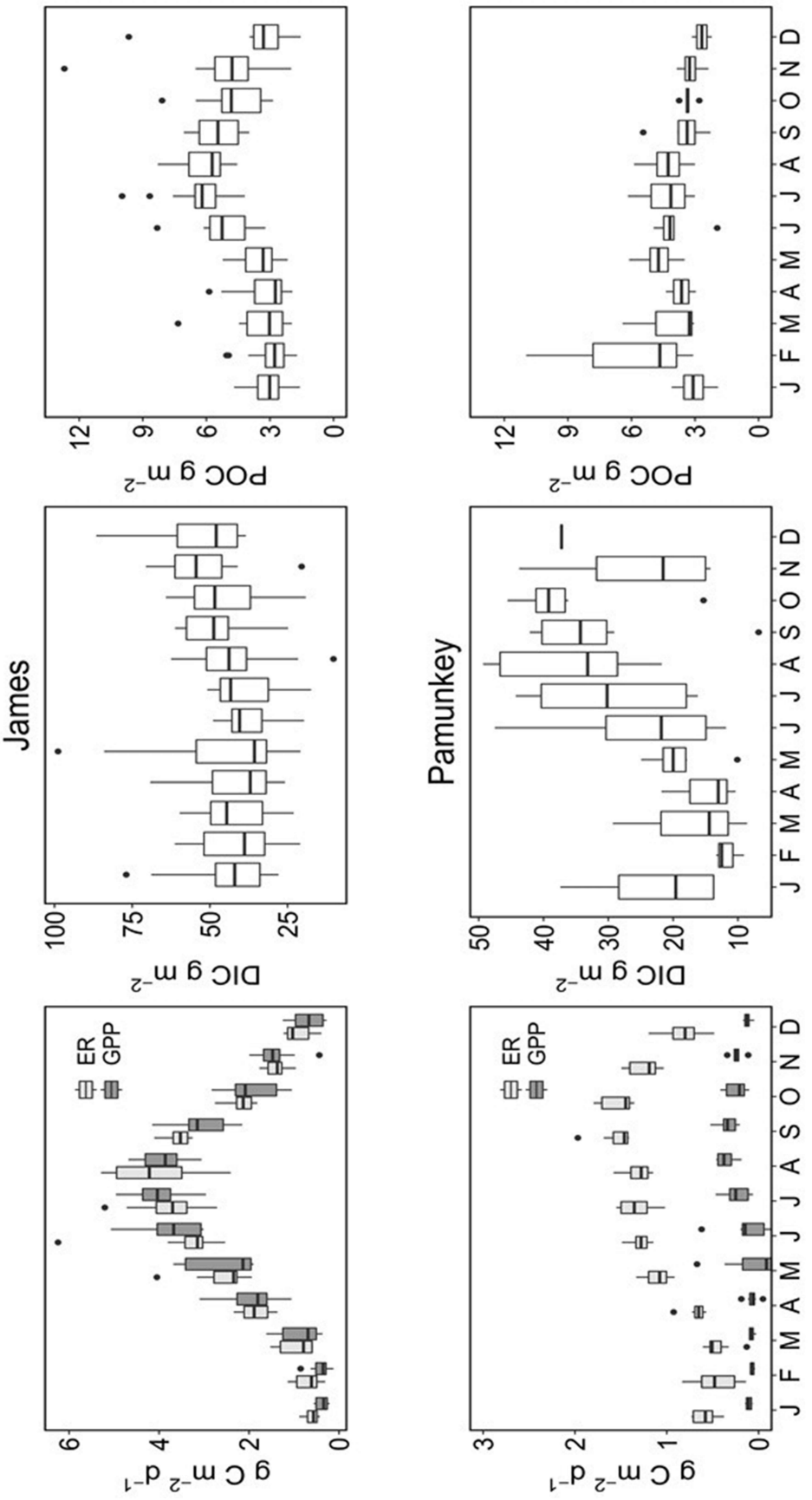

Figure 10. Seasonal variation in ecosystem metabolism (GPP and ER) in comparison to DIC and POC concentrations in the James and Pamunkey estuaries.

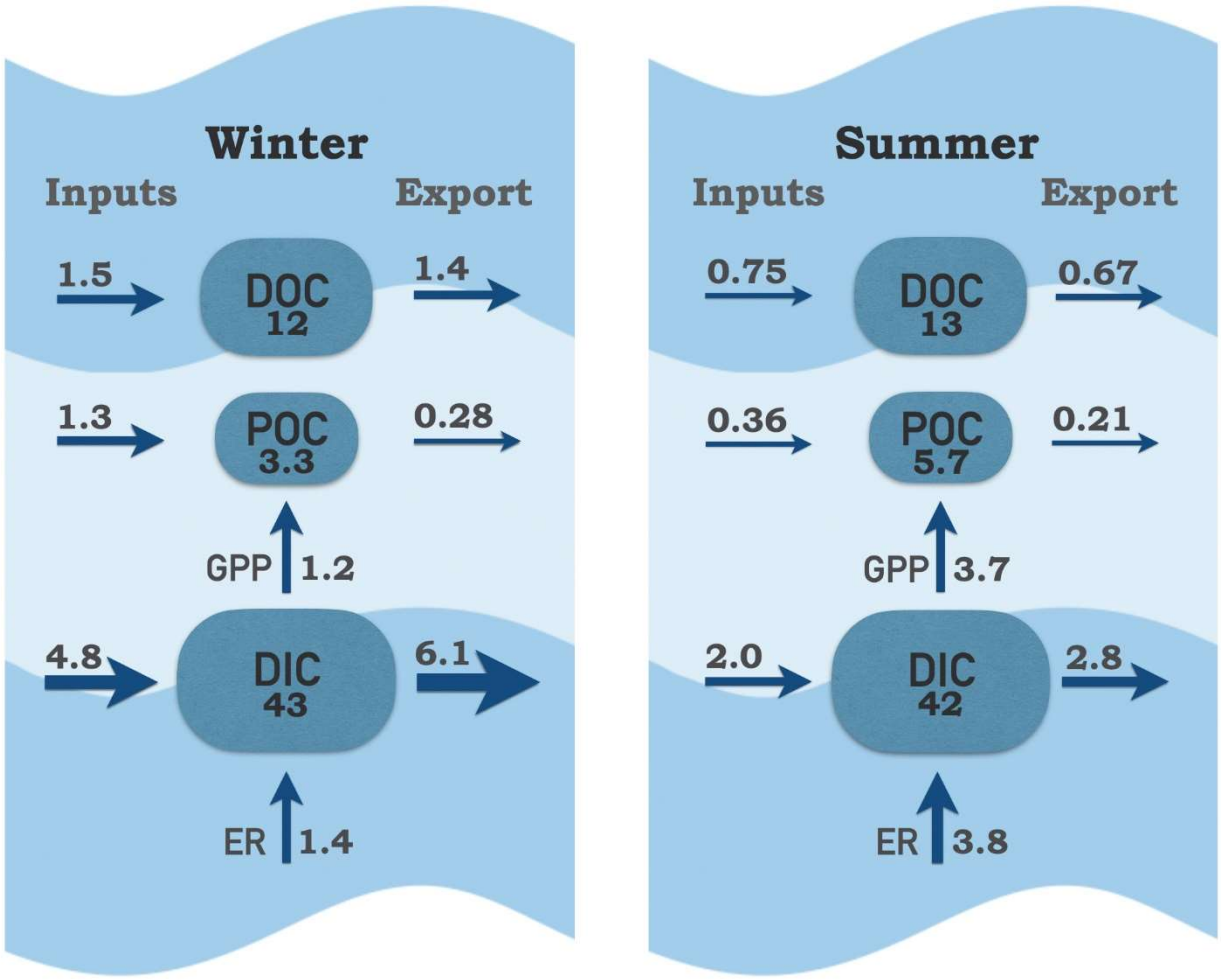

Figure 11. Carbon pools and fluxes within the tidal fresh segment of the James Estuary during winter (Jan-May) and summer (June-Sept). Inputs include riverine, local tributary and point source contributions; exports include tidal exchange and atmospheric losses of CO_2. Carbon pools (boxes) are g C m^{-2}; fluxes (arrows) are g C m^{-2} d^{-1}.